Aus der Kinderklinik und Kinderpoliklinik im Dr. von Haunerschen Kinderspital

Klinik der Ludwig-Maximilians-Universität München

Vorstand: Prof. Dr. Dr. Christoph Klein

Identification of circulation-derived exosomal microRNA candidates for liquid biopsy in pediatric acute lymphoblastic leukemia

Dissertation

zum Erwerb des Doktorgrades der Medizin

an der Medizinischen Fakultät der

Ludwig-Maximilians-Universität München

vorgelegt von

Robert Bartholomé

aus

Bochum

Jahr

2022

Mit Genehmigung der Medizinischen Fakultät der

Ludwig-Maximilians-Universität zu München

Erster Gutachter:	Prof. Dr. med. Irmela Jeremias
Zweiter Gutachter:	Prof. Dr. Klaus Metzeler
Dritter Gutachter:	Prof. Dr. Marcus Hentrich
Mitbetreuung durch den promovierten Mitarbeiter:	Dr. med. Vera Binder
Dekan:	Prof. Dr. med. Thomas Gudermann
Tag der mündlichen Prüfung:	30.11.2022

Table of contents

Zusammenfassung

MicroRNA aus Exosomen -extrazellulären Vesikeln, die auch physiologisch ubiquitär der Zell-Zell-Kommunikation dienen- wurde in vielen Neoplasien als wichtiger Bestandteil der Kommunikation von soliden Tumoren mit ihrer Nische identifiziert. Auch in akuten Leukämien gibt es einige wenige Studien zu dieser Interaktion, aber besonders die Korrelation von exosomaler Beeinflussung und klinischen Verläufen bleibt bislang unbeleuchtet. Da Exosomen in die Blutbahn freigesetzt werden, können Informationen über diese Kommunikation mit einer peripheren Blutabnahme gewonnen werden, einer „liquid biopsy".

In dieser Arbeit wurde die exosomale microRNA-Expression aus peripheren Blutproben von Patienten mit pädiatrischer akuter lymphoblastischer Leukämie analysiert und mit ihren klinischen Verläufen korreliert, um potenzielle „liquid biopsy"-Marker zu identifizieren, schwere Verläufe vorherzusagen und zu verhindern.

Dazu wurden 179 verschiedene microRNAs mit dem „Qiagen miRCURY Focus panel" in 11 Plasmaproben von Patienten sowie von 3 gesunden Kontrollpersonen analysiert.

Beim Vergleich der Proben von therapierefraktären zu therapieansprechenden Patienten, die zum Zeitpunkt der Diagnosestellung und vor Therapiebeginn abgenommen wurden, zeigten die exosomale mir-23b-3p-, mir-409-3p- und mir-7-5p-Expressionen die signifikantesten Unterschiede: Eine Hochregulation von exosomaler mir-23b-3p ($p=0.006$) und mir-409-3p ($p=0.005$) und eine Herunterregulation von exosomaler mir-7-5p ($p=0.003$) in den therapierefraktären Proben.

Diese exosomalen microRNA-Expressionsunterschiede sind vielversprechende Kandidaten für eine „liquid biopsy", um schon bei der Diagnosestellung Patienten zu identifizieren, die von einer vorzeitigen Therapieeskalation profitieren könnten.

Im Vergleich von Patientenproben gegen gesunde Kontrollproben waren die exosomale mir-484 ($p=0.0002$), mir-92a-3p ($p=0.0004$) und mir-25-3p ($p=0.0009$) am signifikantesten hochreguliert.

Um zu beweisen, dass diese Exosomen direkt von den Leukämiezellen stammen, und nicht von anderen „bystander"-Zellen, wurde im Rahmen dieser Arbeit eine neuartige Methode etabliert, in der Exosomen aus dem Serum von „patient derived xenograft"- Mäusen mit akuter Leukämie mit einem anti-CD63-Immunpräzipitationsverfahren humanspezifisch extrahiert wurden. Diese Methode zur Bestimmung der Speziesspezifität und somit der „cell of origin" der Exosomen, zeigte hohe Sensitivität und konnte humane Exosomen bis zur Verdünnung 1:100 von humanem Serum zu Mausserum detektieren.

Mit der Methode konnte gezeigt werden, dass die signifikanten Expressionsunterschiede von exosomaler mir-484, mir-92a-3p und mir-25-3p im Blut von Patienten gegenüber Gesunden direkt durch das Aussenden aus Leukämiezellen bedingt ist. Diese Identifikation der Leukämiezellen als Ursprung ermöglicht weiterführende Studien zur funktionellen Analyse der exosomalen microRNA-

Expressionen und weiterhin Studien zur Identifikation von therapeutischen Zielen gegen die von der Leukämie ausgehenden exosomal-vermittelten Nischenreprogrammierung.

Abstract

MicroRNA derived from exosomes -extracellular vesicles involved in physiological cell-to-cell communication- has been identified as a key component in tumor-to-niche-communication in various solid neoplasias. There is limited data about this communication for acute leukemias, especially the correlation between exosomal reprogramming and the patients' clinical course remains to be investigated. Because exosomes are released in the bloodstream, information about this communication is available via a peripheral venipuncture, a "liquid biopsy".

We analyzed the exosomal microRNA expression from patients suffering from pediatric acute lymphoblastic leukemia and correlated them to the clinical course to identify potential liquid biopsy markers to indicate and prevent adverse courses.

Therefore, 179 microRNAs were analyzed with the Qiagen miRCURY qPCR Focus panel in 11 patients' plasma samples and 3 samples from healthy individuals. When comparing therapy refractory to therapy responding patient samples taken at the timepoint of initial diagnosis prior to therapy, exosomal mir-23b-3p, mir-409-3p and mir-7-5p expression showed the most significant difference with an upregulation of exosomal mir-23b-3p ($p=0.006$) and mir-409-3p ($p=0.005$) and a downregulation of mir-7-5p ($p=0.003$) in the refractory samples.

These exosomal microRNA expression differences represent promising candidates for a liquid biopsy to prevent therapy refraction by escalation of therapy *a priori*.

Exosomal mir-484 ($p=0.0002$), mir-92a-3p ($p=0.0004$) and mir-25-3p ($p=0.0009$) were most significantly upregulated in patients' samples compared to healthy controls.

To prove that these exosomes originate directly from the leukemia cells and not from other "bystander" cells, we established a novel assay using a patient derived xenotransplant (PDX) mouse model. Therefore, we extracted exosomes from PDX mice with acute leukemia human specifically via an anti-CD63 immunocapture. This assay to identify species specific exosomes and therefore the cells of origin of these exosomes revealed high sensitivity, detecting human:mouse serum titrations down to a ratio of 1:100.

With our assay, we confirmed that the significant expression differences of exosomal mir-484, mir-92a-3p and mir-25-3p in patients' blood compared to healthy individuals are directly caused by the leukemia cells. By identifying the leukemia cells as cells of origin, we here lay the groundwork to allow a functional analysis of these exosomal microRNAs and the identification of possible therapeutic targets against leukemia-derived exosome-mediated niche reprogramming.

List of figures

List of abbreviations

Abbreviation	Full form
ALL	Acute lymphoblastic leukemia
AML	Acute myeloblastic leukemia
AraC	Cytarabine
B-ALL	B-cell acute lymphoblastic leukemia
BSA	Bovine serum albumin
cfDNA	Cell-free DNA
CLL	Chronic lymphoblastic leukemia
CML	Chronic myeloblastic leukemia
CTC	Circulating tumor cells
CXCR4	C-X-C chemokine receptor type 4
DNA	Deoxyribonucleic acid
DPBS	Dulbecco's Phosphate-Buffered Saline
EDTA	Ethylenediamine tetraacetic acid
EMT	epithelial-to-mesenchymal transition
ESCRT	endosomal sorting complexes required for transport
GAPDH	Glyceraldehyde-3-phosphate dehydrogenase
GFP	Green fluorescent protein
HPRT1	Hypoxanthine-guanine phosphoribosyl transferase
ILV	intraluminal vesicles
MFI	Mean fluorescence intensity
mir	microRNA
MVB	multivesicular bodies
NK cell	Natural killer cell
NSG	NOD scid gamma
PBS	Phosphate-buffered saline
PCR	Polymerase chain reaction
PDX	Patient derived xenograft
RISC	RNA induced silencing complex
RNA	ribonucleic acid
TAM	Tumor associated macrophages
TEX	Tumor derived exosomes
Treg	Regulatory T-cell
UTR	untranslated region

1. Introduction

B-cell acute lymphoblastic leukemia (B-ALL) is the most common form of cancer in children. Dramatic improvements in therapy regimens and insight in the disease have been made, resulting in an overall survival of over 90% [1]. However, existing risk stratifications miss out some children, since therapy refractory leukemias still require later escalation of therapy and relapses occur [2]. In contrast to initially diagnosed children, relapsed patients have a far worse outcome with only 60% overall survival [3]. Alongside improved therapy of relapsed B-ALL patients, more precise initial risk stratifications are needed. One emerging field in disease characterization is that of “liquid biopsies”, using exosomes to gather more information about the leukemia. Exosomes mediate various processes in leukemia progression, importantly reprogramming of the leukemic niche, resulting in chemoprotection of the leukemic blasts. Little is known whether this exosome-mediated chemoprotection can be used as a diagnostic tool.

1.1 Liquid biopsies: using circulating tumor-derived information for clinical decision making

Many traditional antigen tumor markers (e.g. CEA) detected in blood are currently not recommended for diagnosis and are usually only used for disease progression or therapy success monitoring [4]. However lately, different approaches have been suggested for a precise characterization of disease via analyzing the peripheral blood, so called “liquid biopsies”. Compared to classic biopsies like bone marrow puncture, liquid biopsies show various advantages: Firstly, a venipuncture is far less invasive and as such has less contraindications and complications. Secondly, information of traditional biopsies is always restricted to the actual locus of tissue collection and might not represent systemic disease burden.

Three sources of information are currently mainly investigated to establish liquid biopsies for cancer: circulating tumor cells (CTC), cell-free DNA (cfDNA) and exosomes.

Tumor cells in the bloodstream have been discovered as early as in 1869 by Thomas Ashworth. A minority of CTC have undergone epithelial-mesenchymal transition (EMT), indicating that most cells get in circulation by chance and

without the capability to form metastatic sites [5]. Yet, since CTC reflect the primary tumor sites, they present promising targets for liquid biopsies of several entities of solid cancer [6].

cfDNA is emitted both by healthy and by tumor cells. Consequently, most detection methods rely on the identification of cancer associated mutations and elevated expression of oncogenes [7]. Though cfDNA is thought to derive from dying cells [8], there is evidence that cfDNA plays a pathophysiologic role in cancer via a concept named “genometastasis” [9], which discusses the possibility of transforming non-malignant cells into tumor cells by “transfection” of oncogenes. In pregnancy, the detection of fetal cfDNA in maternal blood is already in clinical use, named “non-invasive prenatal testing” [10].

The presence of exosomes in biofluids and therefore the possibility to extract information in form of a “liquid biopsy” has been a strong driver in the field of exosome investigation. The circulation is a hostile environment for most unprotected potential liquid biopsy molecules, especially for RNA. Exosomes serve as shuttles for these molecules [11]. Taking together the target cell specificity of exosomes via receptor-ligand interaction with the release of exosomes in blood, exosomes are now regarded not only as a mechanism of short distance communication, but also to send information much further throughout the body, even communicating between different organs [12, 13]. In contrast to CTCs and possibly cfDNA, exosomes secretion and the composition of cargo molecules follow tight regulation. Therefore, in contrast to CTCs and cfDNA, exosomes carry not only information about the tumor cells current state, but also indicate ongoing crosstalk and further growth and adaption.

To summarize, the field of liquid biopsies is an active field of investigation, with various possible approaches for information. However, only a fracture of this is already in clinical use.

1.2 Exosomes

Beside various intercellular interaction modi like cytokines and direct receptor-ligand interactions, exosomes present an alternative mechanism of cell-to-cell communication, with their significance both in physiology and in pathology currently revealed by many investigators. Exosomes are nanosized, 40 nm-100 nm sized extracellular vesicles, serving as a carrier for various cargo molecules from the releasing to the recipient cell, where the cargo is taken up and functionally alters the program of the acceptor cell. One of the most investigated exosomal compounds are microRNAs, for which the exosomal membrane

serves as a guarding barrier against degeneration in the otherwise RNase-rich extracellular compartment. Following the discovery that tumor-bearing patients' blood harbors a greater concentration of exosomes than healthy individuals, the role of exosomes in various cancer entities has been investigated. On the one hand, investigators have unveiled the cancer cells' exploit of the physiological communication mode in order to promote tumor growth, metastasis and chemotherapy, on the other hand, possibilities to use exosomes as diagnostic markers and even therapeutic targets emerge from this new field.

1.2.1 Physiology of exosomes

Since the first description of the shed of exosomal microparticles from reticulocytes [14], many aspects of the physiological processes in exosome formation, loading, release and uptake have been discovered. Previously regarded as a mere mechanism of cellular waste ejection, the biology of exosomes is now seen as a targeted and tightly regulated way of sending out specific information.

1.2.1.1 Biogenesis

In contrast to other extracellular vesicles like microvesicles or apoptotic bodies, exosomes are not budded from the cells' plasma membrane, but are of lysosomal origin [15, 16]. When not used for the biogenesis of lysosomes by fusion with endocytotic vesicles, early endosomes mature into so called late endosomes [17]. In late endosomes, intraluminal vesicles (ILV) are formed, differentiating the late endosomes into multivesicular bodies (MVBs) [18]. This process is determined by distinct sorting mechanisms, mainly influenced by the "endosomal sorting complex required for transport" (ESCRT) and its associated proteins TSG-101 and ALIX. Although ESCRT is considered as one of the major players in MVB generation destined for exosome release, ESCRT knockdown does not completely block exosome secretion in cell lines, indicating other pathways. The formation of MVBs via the syndecan-syntenin-ALIX pathway is an alternative to the classic ESCRT-dependent mechanisms [19]. The lipid compound of intraluminal vesicles is also discussed as a protein complex independent structure to conduct the budding of MVBs: Ceramide enrichment in the phospholipid double layer results in a membrane curvature leading to spontaneous formation of the exosome precursors [20]. Möbius et al. even described two populations of MVBs: MVBs destined for exosome release were enriched in membrane cholesterol, whereas a transport to the lysosomes was associated with cholesterol depletion [21].

The enrichment of CD63 is an independent requirement for exosome biogenesis, since its knockout resulted in an impaired exosome release from HEK293 cells [22]. Whether these pathways, especially the ESCRT-dependent and ESCRT-independent ones, exist in parallel or are affecting one another, remains subject to ongoing research [23].

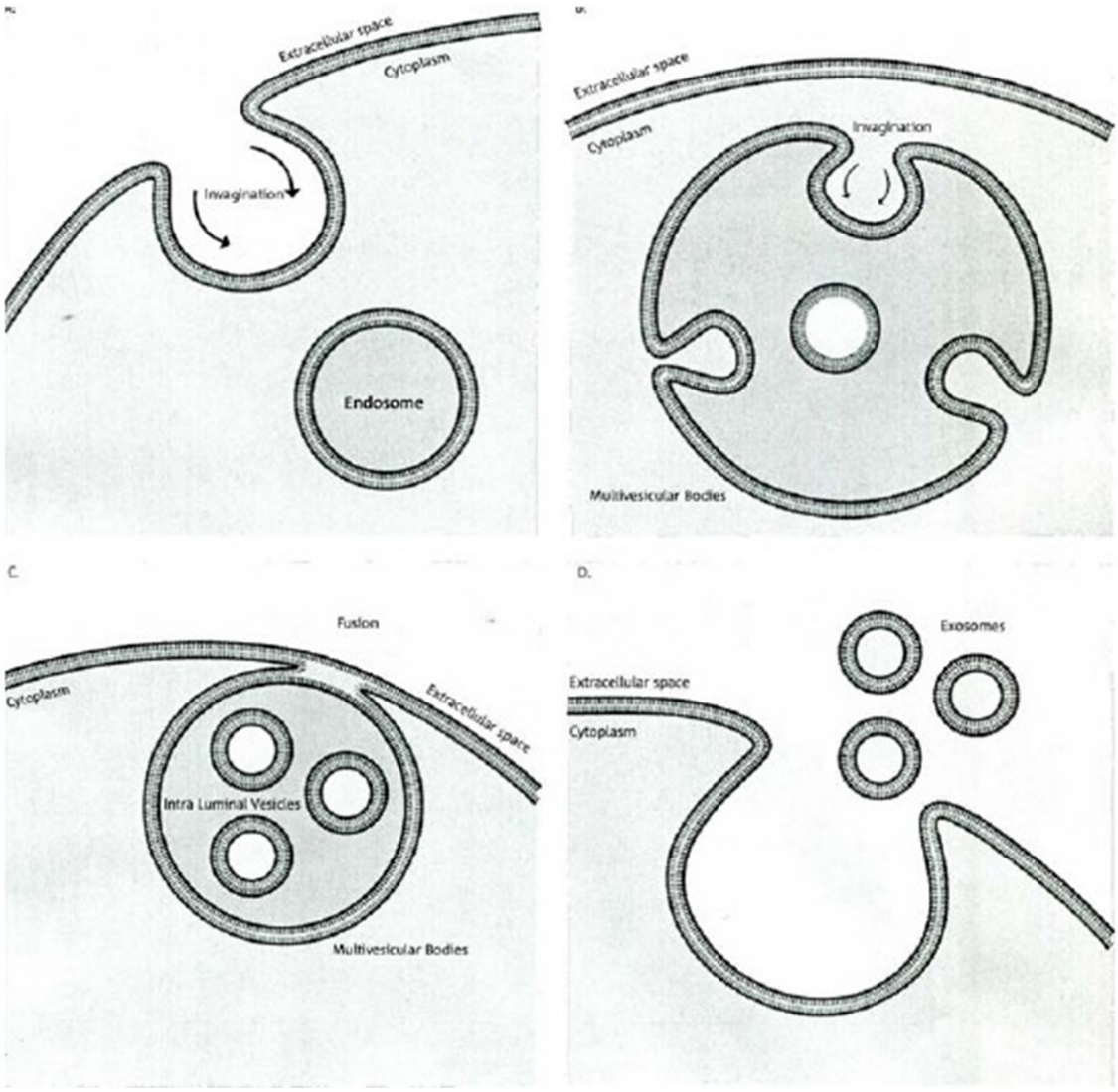

Figure 1: Exosome biogenesis.
Silva et al. 2015 [24]

1.2.1.2 Cargo

In order to function as a mediator of cell-to-cell communication, the exosomes' cargo must be specifically selected to deliver the intended information. Therefore, the loading of MVBs must be specific: The concentration of the messenger molecules is enriched, and unwanted molecules are excluded from the vesicles. To meet these requirements, the content of the intraluminal vesicles is regulated by various import mechanisms:

1.2.1.2.1 Transmembrane proteins

Lipid rafts play an important role in the enrichment of transmembrane proteins. Sphingosine 1-phosphate and G-coupled S1P receptor enrichment in late endosomes leads to a constant autocrine activation of the receptor necessary for enrichment of transmembrane proteins in the forming MVB, especially CD63. [25]

1.2.1.2.2 Packaging of RNA

The RNA size distribution in exosomes is specifically enriched in particles around 200 nucleotides [26]. Beside non-coding small RNA like microRNAs, small nucleolar RNAs and tRNAs, mRNA is present in exosomes [27]. Based on the size distribution, mostly fragments of mRNA are imported into MVBs. Upon further inspection of these fragments, a 3'UTR bias has been discovered [28]. This suggests a non-random packaging of mRNA into MVBs. The 3'UTR fragments were enriched in microRNA binding sites, indicating an interaction between mRNA and microRNA import. Furthermore, an enriched zip code sequence has been investigated to be necessary for the mir-1289 dependent transfer of mRNA to the MVBs [29]. Despite the targeted mechanisms of RNA import, cellular concentration of the imported molecule seems to directly affect the intravesicular concentration, as well: An increase of cellular concentration of specific mRNAs following cellular stress like hypoxia is reflected in the exosomal mRNA levels [30].

MicroRNAs are the most commonly investigated exosome components. MicroRNAs are a class of 20-25 nt long non-coding RNAs, whose primary function is posttranscriptional expression regulation via silencing of mRNAs [31]. From microRNA genes to mature microRNA for exosome export, various maturation steps are necessary. MicroRNA genes are generally found intergenic, in which case a cluster of microRNAs is transcribed polycistronically [32]. The first transcripts, named pri-mirs, are processed in the nucleus by an enzyme complex containing the RNase Drosha [33, 34]. The formed pre-mirs consist of a hairpin structure of around 65 nucleotides. Noncanonically, microRNA genes can also be positioned in the introns of their later targets, linking target and suppressor expression. Here, Drosha is not required, but pre-mirs are cut out by splicing [35]. Pre-mirs are shuttled into the cytosol [36] and again processed by another enzyme, Dicer [37]. The final step results in two mature microRNAs derived from the former hairpin as a duplex, with one 5' and one 3' strand.

Whereas the concentration of total microRNAs in exosomes is upregulated compared to the excreting cell, individual microRNA concentration varies from an accentuated enrichment to non-presence [38]. This indicates a specific mechanism for targeted microRNA sorting into the MVBs and therefore later exosomes. Various features of microRNA import have been pointed out: One suggested mechanism involves the heterogeneous nuclear ribonucleoprotein A2B1 (hnRNPA2B1). In contrast to its cellular counterpart, exosomal hnRNPA2B1 is posttranslationally sumoylated. This modification allows the ribonucleoprotein to bind to a specific microRNA motif (GGAG), enriching the "EXOmotif" containing microRNAs in exosomes. Silencing of the exosomal hnRNPA2B1 lead to a decreased concentration of the EXOmotif microRNAs in exosomes, whereas microRNAs described as "cellular microRNAs" was not influenced [38].

Koppers-Lalic et al. observed an enrichment of 3' uridylation in exosomal microRNA, indicating posttranscriptional modification as another sorting criteria for microRNA import [39].

Interestingly, proteins of the RNA induced silencing complex (RISC), which is necessary for the executive function of microRNAs, also play a role in microRNA enrichment of exosomes. The RISC is not only collocated with the MVBs, but deletion of a key protein, Ago2, leads to an impaired function of the sorting of exosome-typical microRNAs into the ILVs [40, 41].

As a result of the targeted formation and import, the intraluminal vesicles – and consequently the released exosomes - carry distinctive features: a set of enriched surface markers, most notable the tetraspanins CD63 (enriched up to sevenfold on the exosomal surface [42]) and CD81 [43], as well as an intravesicular cargo composition significantly different from the releasing cell's cytoplasmatic concentrations. Especially the enrichment of mRNAs and small RNAs, like microRNAs, stresses the controlled selection of the released molecules. One distinct feature of the exosomal RNA cargo, in contrast to apoptotic bodies and microvesicles, is the absence of ribosomal RNA [44], again stressing the tightly controlled import mechanism.

Upon fusion of the MVB with the cell's plasma membrane, the ILVs are set free as exosomes. Exosomes act as a method of long distance communication, as they are present in biofluids [45-47], most importantly blood [12]. When artificially added to the circulation *in vivo*, labeled exosomes are detectable around 10min in the blood, before being taken up by various organs [48, 49]. Considering the immense stability of exosomes *ex vivo* [50], this indicates the vast turnover time of blood exosomes.

1.2.1.3 Effects on recipient cells

Exosomes can deliver their cargo to the recipient cells using different principles: On the one hand, cells take up exosomes via endocytosis. [51]. On the other hand, a ligand receptor interaction between the exosomes and the recipient cell has been proposed [52]. This mechanism underscores the precision of exosome mediated cell to cell communication: Not only the included information is precisely regulated in the progress of biogenesis, but also the recipient cell type can be predetermined by the exosome's ligand repertoire.

Various studies have investigated the effects of exosomes on recipient cells:

Exosomes' transmembrane components interact with the recipient cells' receptors, inducing an activation of downstream intracellular cascades. For example, B-cell derived exosomal integrins increase intracellular Ca2+ levels in uptaking cells [53]. Transferrin receptor 2, which is colocalized with CD81 on exosomes, mediates MAP-kinase activation, indicating its role as one of the mediators of exosomal cell-cell communication [54]. Immune cell derived exosomes are equipped with functional apoptosis inducing ligands like Fas-ligand, resulting in a cell-independent cytotoxicity against exosome treated cells [55].Chemokines are associated with exosomes to deliver inter-organ information: *In vivo* studies revealed the potency of thymus derived exosomes to induce regulatory T-cells in lung and liver. This effect has been linked to the exosome associated chemokine TGF-β [56].

The acceptor cell is capable of transcribing intact exosomal mRNA into proteins. When incubating non labeled acceptor cells with exosomes containing GFP coding mRNA, the cells gain fluorescence. Even proteins that were not expressed in the acceptor cells were transcribed via mRNA communication [57]. Via this mechanism, the donor cell influences the acceptor cells transcriptome.

Uptaken exosomal microRNA can regulate the transcriptome following the same mechanism as endogenous microRNA: via expression changes in target genes mediated by mRNA silencing [58, 59]. For mRNA silencing, the microRNA ensembles with argonaute proteins to form the RNA-induced silencing complex (RISC) [60]. The microRNA guides the RISC to mRNA containing a complementary sequence, most likely in the 3' untranslated region. [61] Once bound, the target's expression is silenced by degradation of the mRNA via various mechanisms [62]. On the one hand, AGO2 can directly cleave mRNA [63], on the other hand, additional complexes are recruited for deadenylation and decapping [64]. Recently, a non-canonical interaction of microRNA has been

discovered in recipient immune cells: exosomal microRNAs possess the feature to directly bind toll like receptors, resulting in a release of pro-inflammatory cytokines [65]. The manifold physiological functions of exosome-transferred microRNAs have been the target of several research projects. MicroRNA transfer is a universal cell to cell communication tool, influencing for example angiogenesis, cell repair [66], synaptic functions, and even embryonic organogenesis [58, 66-68].

All these findings show that the exosomal cargo remains functional in the vesicles and can alter the cell's program upon its release.

1.2.2 Tumor derived exosomes (TEX)

Patients suffering from neoplastic diseases carry a higher concentration of exosomes in their blood than healthy individuals [69, 70]. Evidence has been presented that upon removal of circulating exosomes by blood ultrapheresis, reduction of tumor size was achieved in tumor metastases [71]. These findings stress the profound influence of exosomes in neoplastic diseases. Tumor cells use exosomes to communicate with each other, transferring resistance mechanisms and oncogenes, as well as with surrounding healthy cells, reprogramming them in order to form a protumoral environment facilitating not only tumor growth, but also metastasis, chemoresistance and immunoescape.

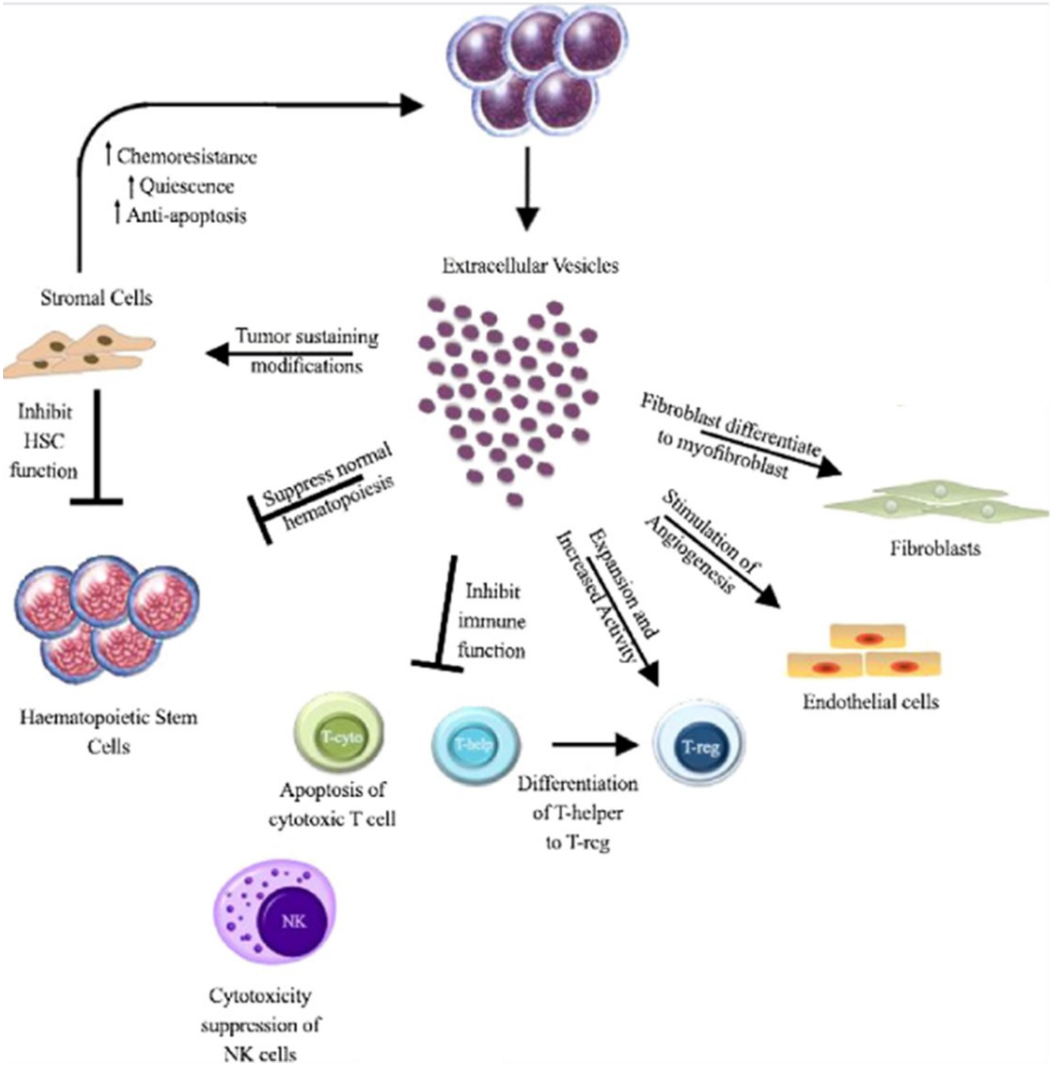

Figure 2: TEX function in cancer and leukemia.
Modified from: Pando et al. 2018 [72]

1.2.2.1 Tumor cells communicate and exchange information via TEX

TEX can be taken up by surrounding tumor cells: horizontal transfer of exosomes from aggressive cells is used to convert less-aggressive cells. The effects in the recipient tumor cell have been named “phenocopying”. Therapy resistant tumor cells alter apoptotic and cell cycle pathways in therapy-sensitive tumor cells, making them less likely to be affected by the therapeutic agent [73, 74]. This has not only been shown for chemotherapy, but also for radiation [75]. Furthermore, exosomes derived from metastatic tumor cells trigger epithelial-to-mesenchymal transition in non-metastatic cells [76]. The transfer of specific exosomal microRNA patterns plays a critical role in this mechanism, but also the direct exchange of oncogenic proteins and drug efflux transporters act as effectors. [77, 78]

As a resistance mechanism independent from other cells, tumor cells shuttle out cytostatic drugs via exosomes, thus evading cytotoxic intracellular concentrations. By treating cell lines with doxorubicin, a correlation in doxorubicin concentration in secreted exosomes and cellular resistance was observed [79]. Additionally, the enrichment of therapy targets on excreted exosomes intercepts the target therapy molecules and lessens therapy effectiveness. This has been shown for breast cancer patients’ serum exosomes, whose surface was enriched in trastuzumab-binding Her2, as well as for B-cell lymphoma excreting rituximab-binding CD20+ exosomes [80, 81]. It is currently not completely understood whether this resistance mechanism is present *a priori* or if it is, at least partially, upregulated in response to therapy.

1.2.2.2 TEX are transferred to bystander cells to alter their function

The tumor cell exosomes are taken up by surrounding non-transformed cells, the tumor-microenvironment, as well as from non-malignant cells in distant body parts reached through circulation. The tumor cells gain various advantages by this healthy cell exploitation, such as an increased level of angiogenesis, induction of metastatic niche formation, protection of the tumor from the immune system as well as the possibility to transform non-malignant cells for tumor progression.

1.2.2.2.1 TEX reduce anti-tumoral immune response

With the help of exosomes, tumor cells that should be identified and attacked by the immune system achieve an immunoinhibiting effect and even exploit func-

tions of the surrounding immune cells, including T-cells, NK-cells, and macrophages.

Findings implicate a systemic weakening of T-cell response to the tumor mediated by secreted exosomes: TEX carry Fas-ligand able to impair the function of T-cells cytokine secretion and induce apoptosis [82]. When incubating CD8+ T-cells with serum, the induction of apoptosis is only observable in T-cells incubated with tumor patients' sera, but not in the cells incubated with healthy volunteers' sera. The level of apoptosis induction is correlated to disease progression [83, 84]. Furthermore, TEX corrupt proliferation of CD8+ T-cells as the physiological answer to IL-2 signaling [85].

In tumor patients' peripheral blood, regulatory T-cells (Tregs) levels are higher compared to healthy individuals. TEX play part not only in the Treg induction, but also in their activation. Here, exosomal TGFβ was found again as the mediator [86]. This benefits the tumor cells, as for example in AML, a low Treg count prior to therapy was correlated with induction chemotherapy response [87].

Natural killer (NK) cells present another threat to the tumor cells. The failure of activation and destruction of the tumor cells has been linked to TEX. Exosomal TGFβ expression downregulates NKG2D, a key receptor for the identification of tumor cells, on NK cells [88]. Since the impairment of NK cells was also found when treating them with patients' sera, a circulation mediated systemic effect is anticipated [89].

Not only do cancer cells use exosomes to impair the immune response against them, but immune cells are exploited as protumoral niche cells, as well. For this, macrophages in the tumor microenvironment are repolarized to form tumor associated macrophages (TAM). Cooks et al. linked tumor-derived exosomal mir-1246 transfer into macrophages with TAM induction [90]. In colorectal cancer, exosomal mir-203 induces TAMs. Here, the induction of TAMs is also correlated to metastasis, underlining the diverse advantages of niche exploitation [91].

In summary, TEX shift the systemic balance of immune cells to a more permitting environment by impairing the function of cytotoxic T-cells and NK cells, while in parallel the function of tumor supportive Tregs and TAMs are upregulated.

1.2.2.2.2 Tumor oxygen requirement induces angiogenesis via TEX

Fast growing tumors are dependent on an equally fast angiogenesis for proper oxygen and nutrient supply. The tumor-controlled angiogenesis is considered

one of the “hallmarks of cancer” [92]. For part of this control, exosomes deliver the key reprogramming information:

A primary effector mechanism to initiate the proangiogenic exosome production is hypoxia [93]. In lung cancer, the mechanisms of hypoxia induced angiogenesis via exosomal mir-494 have been revealed: as response to HIF overexpression, mir-494 enriched exosomes are excreted by the tumor cells to be taken up by endothelial cells. Targeting the phosphatase PTEN, mir-494 mediates the activation of eNOS and hence angiogenesis in the receiving cells [94].

Exosomes transfer activated EGFR to endothelial cells, resulting in activation and autocrine growth stimuli. *In vivo*, Al-Nedawi et al. were able to block exosomal tumor-endothelium communication, upon which they observed an impaired tumor growth and a decrease in neovascularization [95].

Angiogenesis in the tumor microenvironment is dependent on a complex interaction between the tumor and its surrounding cells. Another manner of exosome induced angiogenesis is mediated by stromal myofibroblasts. These tumor-associated stroma cells possess various features important for the promotion of angiogenesis, for example their ability to alter the extracellular matrix composition to an optimal ground for endothelial growth or to recruit immune cells secreting pro-endothelial cytokines [96]. The differentiation of stroma fibroblasts to myofibroblast can be altered by tumor exosomes. Exosomal TGF-β activates intracellular signaling and finally expression of smooth muscle actin in the fibroblasts [97].

The role of exosomes in angiogenesis also highlights their function in inter-organ communication: Expression of tetraspanin CO-029 in circulating TEX facilitates angiogenesis not only on the tumor site, but also distant intestinal organs [98]. Here, the circulating exosomes’ function crosslinks angiogenesis and premetastatic site formation, being both responsible for primary site and metastasis progression.

In conclusion, tumor angiogenesis is facilitated by TEX transporting proangiogenic signals and growth stimuli to endothelial cells.

1.2.2.2.3 Metastasis-promoting TEX induce EMT and prepare a pro-metastatic niche

TEX affect metastatic properties, including the tumor cells’ capability to leave the primary tumor location as well as the priming of a premetastatic niche.

Metastasis initiation at the tumor's original localization is influenced by exosomes: Various studies have investigated the role of exosomes in the induction of epithelial to mesenchymal transition (EMT), one of the principal steps in the metastatic process. In entities like breast cancer and prostate cancer, the uptake of specific exosome-shuttled microRNAs induces EMT-associated pathways and increases the tumor cells migration capability. Strikingly, the exosomes inducing EMT are not secreted by other tumor cells, but by the cells of the tumor microenvironment: tumor-associated macrophages and cancer associated stroma cells, respectively [99, 100]. This clearly underlines the complex niche interaction in the tumor microenvironment. Since these effects require tumor associated cells, it can be argued that the tumor reprograms its microenvironment to serve as a mediator rather than profiting from physiologic niche functions. Here, more functional studies are necessary to understand the mechanisms of exosome mediated EMT in more detail. An unexpected mechanism of metastasis promotion was observed by Ostenfeld et al.: Metastatic properties are gained by excretion of a tumor-suppressor microRNA [101]. This indicates that similar to the excretion of chemotherapeutic agents via exosomes, the purpose of TEX is not only communication, but also elimination of antitumoral endogenous molecules.

Distant body regions are primed by TEX to form a prometastatic environment. This includes angiogenesis, vascular permeability, cell recruitment and composition of the extracellular matrix [102, 103]. By analysis of the targeted cells, mRNA and microRNA transfer have been discovered as the key molecules of reprogramming [104, 105]. The RNA transfer activates metastasis associated pathways in the target cells, like adhesion and oxidative stress response. Interestingly, uptake of tumor-derived exosomes is linked to distinct patterns of integrins on their surface [13]. This finding underlines the model of metastatic organotropism and again highlights the precise regulation of exosome composition in the excreting cells. Nonetheless, it is important to add that premetastatic niche formation remains incompletely understood and that exosomes are not the only resource of priming. For example, the influence of exosomes on the niche relies on CD44, which is associated with cancer initiating cells already present at the premetastatic site [106].

In summary, exosomes participate in metastasis both by mobilizing tumor cells via EMT and by optimizing possible metastatic niches.

1.2.2.2.4 Horizontal transformation of non-malignant cells via TEX oncogene transfer

The horizontal transformation of healthy into malignant cells by TEX has been the subject to scientific discussion: Studies indicate that upon incubation with TEX, non-malignant cells show aggressive tumor-like features, and that this effect is due to the exchange of oncogenic proteins, mRNA and microRNA [107]. For example, the vesicular transport of CML-derived BCR-ABL mRNA into healthy mononuclear cells induces genomic instability [108].

Various votes against this horizontal mechanism of transformation have been expressed, arguing both on a theoretical and practical level. It has been widely accepted that a simple activation or transfer of oncogenes like ras does not transform primary cells but induces cell cycle arrest due to activated tumor suppressors [109]. Additionally, transformed bystander cells would still express various features of their healthy pendants. These cell features are not observed in tumors. Lee et al. have shown that by termination of the exosome transfer, the malignant transformations were transient [110]. So, in contrast to the theory of horizontal transformation, current research suggests a constant but reversible domination of the healthy cells via TEX rather than an irreversible change.

1.3 Childhood B-ALL and niche interaction

In leukemia, blasts repress and replace the healthy hematopoietic cells in the bone marrow. Still, the replacement of healthy hematopoiesis by the leukemic blast must not be understood as the elimination of all other cell types: A variety of non-tumor cells are present in the bone marrow of leukemia patients. Like in the healthy hematopoietic niche, these surrounding non-malignant cells form a complex microenvironment essential for the survival of the leukemic blasts. The leukemic cells are not passive in this interaction, but modify and exploit the niche cells, in order to create a protumoral niche designed for therapy protection and disease progression.

The vast variety and differences of mechanisms and consequences have been subject to research for the chronic and acute leukemias, underlining the specialization of each subtype in niche hijacking [111-113].
The significance of niche interaction in ALL is made clear by the correlation with the clinical outcome: in childhood B-ALL, the recovery rate of leukemic blasts co-cultured with stromal cells is negatively correlated with event-free survival [114].

1.3.1 Niche cells send survival signals to the leukemic blasts

In the physiological hematopoietic system, two distinct niches have been described: The endosteal and the vascular niche [115]. The preference of homing to a specific niche has been reported for B-ALL and AML, whereas in T-ALL no selectivity was observed [116-118]. Applying intravital microscopy, B-ALL cells have been detected to home to the perivascular niche, ousting healthy hematopoietic cells in the process [118]. Nonetheless, the localization of the leukemic cells in the niche appears dynamic and customized to the situation, as new niche localizations emerge during chemotherapy [119]. The importance of the niche sanctuary for the leukemia cells is underlined *in vitro* and *in vivo*: *In vitro*, a cell culture of primary leukemic blasts survives significantly longer when co-cultured with stroma cells [120]. Interestingly, survival was even longer when the stroma cells were derived from B-ALL patients instead of healthy volunteers [121]. *In vivo*, disruption of the leukemia-niche interaction in patients via GCS-F increased leukemia cell apoptosis [122]. The influence of distinct cell types for leukemia survival has been shown, including endothelium, mesenchymal stem cells and osteoblasts [123-125].

1.3.2 Niche cells protect leukemic blasts from chemotherapy

Besides assuring the survival of the leukemic blasts, niche cells play an important role in chemoprotection. Alongside leukemia intrinsic resistance, these mechanisms have become a focus of research in order to understand and undermine protective principles.

A core principle of chemoprotection is the induction of dormancy, impairing the effect of chemotherapeutic agents against proliferation.
Osteoblasts induce dormancy in B-ALL cells. The changes in B-ALL cells close to osteoblasts increase resistance to the chemotherapeutic drug Cytosine arabinoside (AraC) mediated by binding of osteoblastic growth arrest specific 6 (GAS6) to leukemia receptor tyrosine kinases [126]. A further mechanism of osteoblastic protection is the secretion of osteopontin, anchoring the blasts to the extracellular matrix of a protective environment and reducing proliferation [125]. The chemoprotective influence of osteoblast can be inhibited by targeting the ALL cells epigenetic program [127]. This again emphasizes the necessity of a two-sided crosstalk of leukemia cells reorganizing the niche in order to gain chemoprotection.

Another cell type important in niche chemoprotection is the mesenchymal stem cell. Direct adhesion between these cells and B-ALL cells via very late antigen-4 (VLA-4) on the leukemia and vascular cell adhesion molecule (VCAM) on the MSCs plays a role in protection, blockage of this axis leads to an increased sensitivity to chemotherapeutics [128]. This was also shown *in vivo* using an antibody against the integrin α4 in VLA-4, natalizumab [129]. In childhood B-ALL patients, high VLA4 is linked to poor prognosis [130].
Furthermore, adhesion via β1-integrin to the niches' extracellular matrix weakens doxorubicin induced apoptosis. The mechanism of this chemoresistance depends on β1-integrin-fibronectin-interaction, inhibiting pro-apoptotic proteins like caspase-3 and upregulating the expression of apoptosis-inhibitors like XIAP [131].

For the homing and survival of both healthy hematopoietic stem cells and leukemic blasts, interaction with the bone marrow stroma cells via the CXCR4/CXCL12 (SDF-1) axis is essential [132].
CXCR4/CXCL12 has also been discovered as an important mediator of the previously described chemoprotective mechanisms:
Increased levels of CXCL12 amplify VLA-4/VCAM adhesion [133]. A higher expression of CXCR4 on leukemic cells increases interaction with the stroma and has been linked to resistance to chemotherapy induced apoptosis as well as with patients' poorer prognosis [134, 135]. Various studies have tried to overcome niche mediated chemoprotection by disruption of the CXCR4/CXCL12 axis [136]. Plerixafor, a CXCR4 antagonist, is an approved drug for peripheral blood stem cell mobilization. In childhood B-ALL, first clinical trials have started to evaluate its benefits not in mobilizing healthy hematopoietic cells, but in disrupting leukemia blasts from their safe microenvironment in order to enhance the effect of chemotherapy [137].

The role of galectin-3 in chemoprotection has also been investigated on a mechanistic level. In isolated acute leukemia cells, galectin-3 levels do not differ from those of healthy hematopoietic cells [138]. In coculture, stroma derived galectin-3 is shuttled to B-ALL cells both as a soluble factor and in exosomes [139]. In the leukemic cells, it induces both an autoinduction of galectin-3 production as well as activation of the Wnt-pathway, upregulating survival genes like survivin and c-myc. The increased galectin-3 levels in B-ALL cells induce chemoresistance against multiple drugs, including vincristine and tyrosine-kinase inhibitors [140, 141]. Galectin inhibitors reverse this chemoprotection and are under research as novel therapeutic strategies [142, 143].

Additionally, more direct responses to specific therapeutic agents have been found. Asparaginase, a drug commonly used in the treatment of ALL, deprives the leukemic cells form Asparagine. Mesenchymal stem cells secrete high levels of asparagine, providing the leukemia with the needed amounts and therefore impairing therapy effects [144]. The same effect has been described in bone marrow adipocytes, upregulating glutamine *synthetase* in response to chemotherapy [145]. Since obesity is a risk factor for relapse, it can be argued that this effect is likely not limited to the bone marrow, however, total glutamine levels in the plasma of diseased children remains unchanged, indicating that not all adipocytes, but rather a subfraction of adipocytes in the bone marrow contributed to a local rather than systemic antitherapeutic effect [145, 146]. Insulin-like growth factor binding protein 7 (IGFBP7) mediates increased asparagine and glutamine synthesis activity. ALL cells played an essential role in the regulation of secretion of IGFBP7, indicating an active reprogramming of the niche rather than exploitation of already established principles [147].

The bone marrow niche does not only protect ALL cells form classic chemotherapeutic agents, but also against antibody-based therapies. It was shown that the tumor microenvironment cannot prevent antibody binding, but by secreting PGE2 are able to keep away macrophages and thus inhibiting phagocytosis mediated killing of the leukemia cells [148].

1.3.3 Niche interaction can be used to optimize chemotherapy

Analysis of the microenvironment-leukemia interaction can be used to find the best suited therapy, as shown by Zhihong et al. targeting AML cells. By comparing the activation of various intracellular pathways using proteomics in leukemic cells cultivated with or without stroma cell support, it was made possible to determine the most effective combination of signaling inhibitors [149]. This proves the principle that the niche cells' chemoprotection does not only present a new target for antileukemia therapy, but that this therapy can be optimized by leukemia-niche interaction analysis.

1.3.4 The role of exosomes in leukemia-niche interaction

Rather than just using the physiological mechanisms of the hematopoietic niche, leukemia profoundly converts the niche cells to form a supportive, promotive, and protective microenvironment for its own advantage. For this, the leukemic blasts must deliver information to the surrounding cells. Comparing the

MSCs from leukemia infiltrated bone marrow against MSCs from healthy bone marrow, the leukemia influenced MSCs showed significant functional alterations, like a decreased ability to support healthy hematopoiesis, but did not acquire any genetic alterations [150]. In MDS, MSCs have been shown to acquire epigenetic and transcriptomic changes rather than genetic ones [151]. Thus, the influence of the leukemic blasts is most probably not achieved via a permanent transformation of the niche cells, but by a constant reprogramming.
Different mechanisms of crosstalk have been proposed and experimentally affirmed: Secretion of chemokines, especially growth factors or the direct transfer of molecules and even mitochondria via nanotubes connecting the leukemic cells to the niche cells [152].
In addition, more and more evidence points out the role of leukemia derived exosomes in the reprogramming of the niche.

Leukemia derived exosomes alter differentiation programs in the bone marrow niche cells, urging the cell into a more leukemia than healthy hematopoietic cell supporting state. For example, stroma cells differentiate into cancer-associated fibroblasts when exposed to leukemia derived exosomes, whereas the exposure of endothelium to leukemia derived exosomes increases angiogenesis [153]. These alterations are observed both in niche cells cocultured with leukemia cells and in niche cells only incubated with leukemia derived exosomes [154]. In CLL, leukemia cells show both elevated levels of engraftment and proliferation in a xenograft model when cotreated with leukemia derived exosomes [153]. Exosome shuttled microRNA as the key component of the TEX-mediated reprogramming has been identified, for example in AML-to-endothelium niche interaction [155].

For B-ALL, data about the reprogramming of the microenvironment via exosomes is limited. Nonetheless, it has been observed that B-ALL derived exosomes switch the niche cells metabolism to decrease oxidative glycolysis in order to produce and excrete lactate [156]. It has been suggested that the lactate can be taken up by the ALL cells as a source of energy. This argument is underlined by the observation of a reciprocal microenvironment-mediated metabolic switch in the ALL cells, impairing their own production of energy, but resulting in chemoprotection [157, 158]. These findings enhance the hypothesis that leukemia to niche crosstalk via exosomes is also a key mediator of resistance in B-ALL.

2. Hypothesis and aim

Evidence grows that B-ALL cells hijack their niche in order to form a chemoprotective microenvironment. The emerging role of leukemia derived exosomes in this process is becoming clear. As one of the principal cargo molecules of exosomes, microRNAs are important candidates to mediate the chemoprotective mechanisms.

It was shown that the reprogramming of the niche cells via exosomes has variable effectiveness depending on the delivered microRNA expression levels, resulting in a different level of chemoprotection and thus different level in therapy response, with the most effective reprogramming leading to therapy refractory cases and relapse.

We hypothesize that leukemias that were refractory to chemotherapy exploit their surroundings more effective/via different signaling pathways and that we can detect these differences by analyzing the leukemias' exosomal microRNAs.

Since niche reprogramming already starts prior to chemotherapy and exosomes are secreted in the circulation, we hypothesize to find these expression differences in patients' blood at the timepoint of diagnosis.

We aim to identify a pattern of B-ALL patients' blood tumor-derived exosomal microRNA expression that can be found at diagnosis indicating strong niche reprogramming and therefore high risk for relapse with the need of therapy escalation/modification. These expression profiles will represent promising biomarkers to be tested in addition to risk stratifications in the form of a liquid biopsy, as well as interesting therapeutic targets.

3. Material and methods

3.1 Material

3.1.1 Instruments

Function	Name	Vendor
Spectrometer	Nanodrop OneC	Thermo scientific
Centrifuges	5424R & 5417C	Eppendorf
Vortex	Vortex Genie 2	Scientific industries
qPCR cycler	Lightcycler® 480 II	Roche
pH meter	H1221	Hanna instruments
Flow cytometry	LSRFortessa X-20	BD
Scale	PCB 250-3	Kern
Micro scale	ABJ 220-4M	Kern
Ultracentrifuge	TL-100	Beckman coulter
Gel electrophoresis system PCR	Gelsystem Mini S	PerfectBlue™
PCR transformator	Basic power supply	PowerPac™
Cell counter	Countess™ Automated Cell Counter	Invitrogen
Magnetic stand	Magnetic stand 96	Invitrogen
Capillary RNA electrophoresis	Bioanalyzer	Agilent
Gel documentation	EBox Vx2	Vilber lourmat
PCR thermocycler	ProFlex PCR System	Applied Biosystems
Shaker	KS125basic	IKA Labortechnik
Tube roller	RM5.40	Karl Hecht

3.1.2 Software

Function	Name
Tm calculator	New England biolabs Tm calculator
Primer alignment	APE
Flow cytometry readout	FlowJo

Statistics and figure design	GraphPad prism
Algorithm for single miRNA normalization genes	NormFinder excel add-on

3.1.3 Reagents and buffers

Name	Vendor
Dulbecco's PBS (1x)	Gibco
Ethanol	Roth
Isopropanol	
Glycine	
Bovine serum albumin	Sigma
Chloroform	Sigma-Aldrich
FACSClean	BD
UltraPure™ Agarose	Invitrogen
TRIzol	
UltraPure™ glycogen	
Aldehyde/Sulfate Latex Beads	
Dynabeads™ M-450 Epoxy	
Midori green	Nippon genetics
Gene ruler mix	Thermo scientific
dNTP mix	
GoTaq® DNA Polymerase	Promega
GoTaq buffer	
Ficoll-Paque	GE Healthcare - Life Sciences

3.1.4 Commercial kits

Function	Name	Vendor
cDNA synthesis	QuantiTech Reverse Transcription Kit	Qiagen
qPCR cDNA synthesis	miRCURY LNA RT kit	
qPCR	miRCURY LNA SYBR green PCR kit	
Exogenous qPCR controls	RNA spike in, for RT	
Automated RNA electrophoresis	Bioanalyzer RNA pico chip	Agilent

3.1.5 Buffers

Name	Composition
Dynabeads coupling buffer	Buffer 1: 0.1 M sodium phosphate pH7.4 Buffer 2: DPBS +0.1%BSA 0.22µm filtrated plus 2mM EDTA
Isolation buffer	DPBS+ 0.1%BSA 0.22µm filtrated
TAE buffer (50x)	10.8 g TRIS Base, 1.14 ml acetic acid, 0.7 g EDTA, ad 1 l H2O
Low pH washing buffer	25mM phosphate citrate pH 5, 0.22µm filtrated

3.1.6 Serum

Name	Lot#	Vendor
Normal mouse serum	#SE252031	Invitrogen
	#UA276776A	

3.1.7 Antibodies

Target	Clone	Vendor
CD63	H5C6	Novusbio
	H5C6 (PeCy7)	Invitrogen eBioscience
	MX-49.129.5 (Alexa fluor 647)	Santa Cruz Biotechnology
CD81	JS-81 (APC)	BD Pharmingen
Isotype control	Mouse igG1 kappa isotype (PeCy7)	Invitrogen eBioscience

3.1.8 Primer

Target	Forward sequence	Reverse sequence
GAPDH	TCGGAGTCAACGGATTTGGTCGTA	ATGGACTGTGGTCATGAGTCCTTC
HPRT1 [159]	ATCAGACTGAAGAGCTATTGTAATGACCA	TGGCTTATATCCAACACTTCGTG
CXCR4 [160]	GCGTGTAGTGAATCACGTAAAGC	CTATACCACTTTGGGCTTTGGTTAT

3.1.9 MicroRNA primer

Function	Name	Vendor
qPCR panels (14x179 microRNAs)	miRCURY LNA focus panel serum/plasma	Qiagen
Target microRNAs	hsa-mir-484 assay	
	hsa-mir-25-3p assay	
	hsa-mir-92a-3p assay	
Normalization microRNAs	hsa-mir-151a-5p assay	
	hsa-mir-532-5p assay	
	hsa-let-7d-3p assay	
	U6 snRNA	

3.2 Methods

3.2.1 Patient samples

All patients and/or their custodial gave consent to sampling, storage of the samples in a biobank and usage for research.

3.2.2 Patients and healthy individuals' plasma isolation via Ficoll-Paque protocol

All pediatric B-ALL patients' blood samples were collected and processed at the clinic and transferred frozen to the laboratory. Healthy controls blood samples were collected by venipuncture in EDTA coated monovettes and processed in the laboratory, following the same protocol used for the patient samples. For plasma isolation, around 20 ml of blood was filled up with PBS to 35 ml and lay-

ered on top of 15 ml Ficoll-Paque in 50 ml Falcon tubes. For separation of cells and plasma, the samples were centrifuged at 800 g for 30 min with minimal brake setting. Plasma was carefully aspirated, leaving ~10% to avoid cell carry-over. All samples were stored at -80°C prior to processing.

3.2.3 Serum of PDX mice

Serum was taken from full-blown leukemia PDX NSG mice as well as from non-injected NSG mice. For this, the mice's' hearts were punctured immediately after euthanizing them. All blood was collected in 1.5 ml centrifugation tubes and allowed to coagulate for 30 min up to 1 h. Centrifugation for 10 min at 1500 g separated the serum from coagulated material. Serum was collected, leaving ~10% of the volume to avoid cell carry over. When the serum did not seem clear, centrifugation was repeated. All PDX sera were collected by trained technicians and stored at -80°C. With this protocol, 100 µl to 400 µl serum was collected per mouse. If needed, serum from different mice, that were transplanted with primary cells from the same patient, was pooled.

3.2.4 Fish serum

Immediately after euthanasia, zebrafish hearts were punctured with a small canula. Blood was collected in a 1.5 ml centrifugation tune and coagulated for 1h at room temperature, followed by centrifugation for 10 min at 1500 g. The fluid supernatant was collected leaving a small amount of serum on the pellet to avoid cellular contamination. Because one fish only yielded a few µl of blood, ~20 fish were pooled for 100 µl of zebrafish serum.

3.2.5 Preclearing of serum/plasma samples

All serum and plasma samples were first sequentially centrifuged at 2000 g for 15 min followed by 12.000 g for 30 min at 4°C. Respective supernatants were kept, whereas the first pellet containing leftover cells and apoptotic bodies as well as the second pellet containing large extracellular vesicles, such as microvesicles, were discarded.

3.2.6 Ultracentrifugation

For ultracentrifugation, the samples were transferred to 1 ml ultracentrifugation tubes. The volume was adjusted to 1 ml with PBS and weight was equilibrated on a microscale allowing a derivation of 0.001 g. Ultracentrifugation was performed with a TLA-100 rotor at 40,000 rpm for 1.5 h at 4°C. Since the exosomes did not form a visible pellet, the assumed place of the pellet was marked prior to removing the ultracentrifugation tubes from the rotor. Supernatant was removed carefully in two steps: First, 900 µl, then 95 µl supernatant was taken off very carefully, to not manipulate the pellet with the pipette tip. Approximately 5 µl of volume was left on the exosome pellet as safety measurement.

To achieve higher purity of exosomal material and remove any non-vesicular contamination, the first ultracentrifugation's pellet was resuspended in 1 ml PBS and ultracentrifuged again applying the same centrifugation speed and time.

3.2.7 Hydrophobic capture of exosomes enriched by ultracentrifugation

The pelleted purified exosomes were bound to latex beads by a protocol slightly modified from Théry et al. [161]: The exosomal pellet was incubated with 20 µl of PBS and 10 µl (0.4 µg) of latex beads over night at 4°C with constant mixing of a tube roller. The next day, sample volume was brought up to 300 µl with PBS and incubated additional 2 hours at room temperature. Beads were pelleted by centrifugation at 7000 g for 3 min to remove the non-bound ultracentrifugation pellet content in the supernatant. Excess aldehyde groups on the latex beads were blocked with 500 µl of 100 mM glycine for 30 min; unspecific protein binding was blocked by washing the beads three times with BSA. For this, beads were pelleted by centrifugation at 7000 g for 3 min; after every centrifugation, the supernatant was exchanged with 500 µl PBS with 0.1% BSA.

Hydrophobic latex bead bound exosomes were stained with different antibodies following the vendor's recommended dilution for 1 h in the dark with constant agitation, followed by three washes in PBS with 0.1% BSA to avoid carry-over of unspecifically bound or free antibody. Fluorescence levels on the beads were measured with the LSRFortessa; all flow cytometry data was analyzed with the FloJo software.

3.2.8 CD63-anitbody tests

For human cells, Nalm6 cell line cells were used. For murine cells, peripheral blood cells of control mice were isolated following a routine Ficoll-Paque proto-

col. Briefly, 1 ml of whole murine blood diluted in 2 ml PBS was centrifuged at 400 g for 20 min through 1 ml of Ficoll. The mononuclear cell layer above the Ficoll was carefully aspirated and washed once with PBS.

1 million cells per sample were pelleted and stained by resuspending in either antibody or isotype control solution (0.5 µg antibody per 1million cells). After incubation for 45 min at room temperature protected from light with constant shaking at 500 rpm, cells were pelleted by centrifugation (400 g for 5 min) and washed twice in PBS. All samples' fluorescence was measured at the LSR Fortessa; data was analyzed using the FloJo software.

3.2.9 Coupling of immunomagnetic beads

The anti-CD63 capture antibody H5C6 was covalently coupled to the epoxy group-carrying magnetic beads following the protocol recommended by the supplier. In short, 250 µl beads were washed two times in a 0.1 M sodium phosphate buffer, making use of their magnetic properties by pelleting the beads on a magnetic stand in between the washing steps. Washed beads were incubated with 50 µl (1 mg/ml) of the unconjugated anti-CD63 antibody H5C6 for 15 min alone in a total coupling volume of 250 µl, then over night at room temperature after adding fetal bovine serum (final concentration c=0.1% w/v) to block excess epoxy groups. After washing-out the remaining free antibody with three 1 ml DPBS +0.1% BSA wash steps, beads were adjusted to a concentration of 1 x 10^7 beads/ml in DPBS with 0.1%BSA and 2 mM EDTA and stored at 4°C.

3.2.10 Isolation of CD63+ exosomes

Precleared serum was incubated with anti-CD63 H5C6 coupled magnetic beads at 4°C in low-stick centrifugation tubes. The incubation step was performed over night to allow optimal antibody-antigen interaction. Due to the magnetic capacities of the beads, bead-CD63+-exosome complexes can be pelleted and washed on a magnetic separator. For this, the incubated samples were transferred in a protein low-binding 96-well plate and put on a 96-well magnetic stand for 2 min. Supernatant was removed carefully from the opposite side of the pellet in order to keep loss of exosomes minimal. After removal of the exosome depleted serum supernatant, the anti-CD63 beads were washed with 300 µl PBS/0.1% BSA as well as two times incubated for 10 min in a low pH citrate

buffer to eliminate non-specific binding. Washed CD63+-exosome-coupled beads were immediately processed in subsequent experiments.

3.2.11 Cytometry analysis of bead-exosomes complexes

Bead-bound CD63+ exosomes were characterized via FACS by detection of the established exosomal surface marker proteins CD63 and CD81. The washed, serum-incubated beads were magnetically pelleted and stained with the detection antibodies in recommended concentrations (5 µl of antibody solution per 100 µl for anti-CD63, 20 µl of antibody solution per 100 µl volume for anti-CD81) for 1 hour at room temperature protected from light with constant shaking at 500 rpm. Excess detection antibody was washed out by magnetically pelleting the beads and discarding the antibody solutions, followed by two wash steps with 300 µl isolation buffer. Beads were resuspended in 200 µl PBS for flow cytometry. All samples were measured at the LSRFortessa and data was analyzed using the FloJo software.

3.2.12 RNA isolation

Exosomal RNA was isolated using the TRIzol reagent following the vendor's instructions. All steps were performed in low-binding, RNAse free centrifugation tubes. 750 µl TRIzol was directly added on the ultracentrifugation- or bead-enriched exosome pellet. After 5 min incubation, 150 µl pure chloroform was mixed in. Following a 3 min incubation at room temperature, samples were centrifuged at 12,000 g for 15 min at 4°C to separate RNA, DNA and protein phases. The upper aqueous phase containing the RNA was aspirated, leaving a small fraction in the tube to minimize the risk of DNA and protein carry-over. Because of the estimated low total amount of exosomal RNA in the samples, 20 µg of glycogen was added as a carrier to both give a visible pellet and reduce RNA loss on tube and pipette surfaces. RNA was precipitated by adding 375 µl isopropanol, followed by a 10 min incubation at room temperature. The RNA pellet was pelleted at 12,000 g for 10 min at 4°C and washed with 70% Ethanol to clear carry-over TRIzol remains. By pelleting the washed RNA at 12,000g for 10 min and air-drying the RNA pellet for 10 min, all ethanol was removed from the RNA pellet. A final volume of 6.5 µl RNAse-free H2O was used for resuspension of RNA facilitated by a 10 min heating of the samples to 55°C. Immediately after heating, RNA samples were vortexed, shortly spun down and put on ice for short term storage or stored at -20°C over night.

3.2.13 RNA capillary electrophoresis

Exosomal RNA size distribution was determined by automated RNA capillary electrophoresis using RNA pico chips on the Agilent Bioanalyzer. No modifications were made to the recommended protocol. In brief, a chip was prepared by filling the wells with 9 µl of a gel-dye mix with the help of an attached plunger, adding 5 µl RNA marker in each well, 9 µl of a conditioning solution and 1 µl of RNA ladder solution in the predetermined wells. 1 µl of the RNA samples was pipetted in each sample well. The prepared chips were vortexed for 30 seconds and immediately read out at the Agilent Bioanalyzer instrument, using the “mRNA pico” program, which calculates the percentage of rRNA contamination and is therefore beneficial for exosomal RNA quality control.

3.2.14 PCR analysis of exosomal mRNA

TRIzol isolated exosomal RNA was reverse transcribed into cDNA with the QuantiTect reverse transcription kit by Qiagen. Since RNA concentration was too low to be measured by the Nanodrop spectrometer, the total sample volume was used in the cDNA reaction mix without further dilution. All pipetting steps were performed on ice. The kit contains a DNase step prior to reverse transcription. For this, the RNA samples were mixed with 2 µl of DNase master mix and RNAse free water in a total volume of 14 µl and incubated for 2 min at 42°C in the ProFlex PCR System thermocycler. For reverse transcription, 1 µl of reverse transcriptase, 1 µl of random primers and 4 µl of RT buffer was added to the samples. The cDNA synthesis reaction was incubated at 42°C for 15 min, followed by a 3 min heat inactivation of the RT enzyme at 95°C. After reverse transcription, cDNA samples were diluted with RNAse-free H_2O to 100 µl and immediately put on ice.

For polymerase chain reaction, the GoTaq *Thermus aquaticus* polymerase system was used. In order to prevent further dilution of the exosomal cDNA, maximal sample volume was added in the reaction mix. The 50 µl reactions consisted of 10 µl reaction buffer (5x), containing 7.5 mM Mg_2Cl, 0.5 µl GoTaq polymerase (1:100), 0.5 µl dNTPs (1:100), 1.6 µl of forward and reverse primers (1:33) and 36 µl cDNA.

PCR reaction was performed with the ProFlex PCR System thermocycler. Annealing temperatures for the respective primers were calculated with the New England Biolabs Tm calculator.

GAPDH primers

Step	Temperature/°C	Time/sec
Initial denaturation	95	60
35 cycles of		
denaturation	95	60
annealing	56	30
Elongation	72	30
Final extension	72	120

CXCR4 primers

Step	Temperature/°C	Time/sec
Initial denaturation	98	60
35 cycles of		
denaturation	98	30
annealing	52	30
Elongation	72	15
Final extension	72	120

HPRT1 primers

Step	Temperature/°C	Time/sec
Initial denaturation	94	60
35 cycles of		
denaturation	94	30
annealing	55	30
Elongation	72	30
Final extension	72	300

Gel electrophoresis in a 2% agarose gel was used for visualization of the amplicons. For this, 1 g of agarose was heated in 50 ml of 1xTAE buffer until all agarose crystals were dissolved. Before casting the gel, 5 µl Midori green, an intercalating dye used as a non-toxic alternative to ethidium bromide, was added to the liquid agarose. After letting the agarose harden at room temperature on a gel tray equipped with a 10-well comb, the comb was removed, and the tray transferred to a PerfectBlue™ Gelsystem Mini S filled up with 1xTAE buffer. Since the GoTaq PCR reaction buffer already contains a loading dye as well as glycerin, samples were directly loaded on the gel. To identify the correctly sized amplicons, 5µl of the GeneRuler DNA Ladder Mix, which contains predefined DNA fragments in the length from 100 to 10k base pairs, was used. Gels were run for approximately 45 min at 100 V. Images were created by visualizing the fluorescence of the intercalated Midori green in the double-stranded amplicons with a gel documentation station using the automatically generated exposure settings.

3.2.15qPCR analysis using the miRCURY focus panels

All primary patients' and healthy volunteers' plasma samples were thawed on ice, precleared and ultracentrifugated as described above. RNA extraction via TRIzol was performed as described above. All ultracentrifugation and RNA extraction steps were run in triplicates to minimize technical variations. RNA elutions were then mixed and used for a single cDNA synthesis step. 750 µl TRIzol solution was directly added on the ultracentrifugation pellet. For quality control of all steps, 1 µl of synthetic spike-in RNA (called UniSp2, UniSp4 and UniSp5) was added to the mixture prior to adding the chloroform. For the cDNA synthesis, a total reaction volume of 20 µl consisting of 13 µl RNA, 1 µl UniSp6 spike-in, 2 µl enzyme solution and 4 µl reaction buffer was used. The synthesized cDNA was frozen at -20°C for a maximum of 4 weeks.

For qPCR analysis, all samples and reagents were thawed on ice. Per sample, 20 µl of cDNA was mixed with 1000 µl of SYBR green dye as well as 98 µl RNAse-free water and transferred to the two Focus panel 96-well plates containing the lyophilized microRNA primers. 10 µl of the mix was added per well using a multi-channel pipette with repeated pipetting to properly dissolve lyophilized primers. The plates were shortly spun down and incubated for 5min to assure optimal primer dissolving, followed by the light cycler read-out using the settings adopted from the vendor's protocol:

Step	Temperature/°C	Time/sec	Data acquisition
Initial heat activation	95	120	
45 cycles of			
denaturation	95	10	
Annealing/ Elongation	56	60	Single Fluorescence signal
Melting curve analysis	60-95		Continuous melting curve analysis

3.2.16 Data analysis of the miRCURY Focus panel data

Raw Cq data for all the panels microRNAs were calculated by the Roche Light cycler software using the “2nd Derivative max” quantification method. From these, all values >39,0 cycles were excluded. For quality control for the technical steps of RNA isolation to qPCR, the Cq values of the spike-ins were assessed as followed:

1. All spike-ins were amplified in the runs

2. Cq(UniSp2)>Cq(UniSp4)>Cq(UniSp5)

3. The inter-plate calibrator UniSp3 (6 replicates per sample) had no Cq difference >0,3.

In contrast to the qPCR analysis of cellular microRNA, in which the small nuclear RNA U6 is used as a housekeeper for data normalization, no universal housekeeper is known in exosomes. Instead, housekeepers must be determined for each study and starting material respectively. The best method when analyzing a large number of extracellular microRNAs is to normalize against the mean of all the panel’s microRNAs [162]. Following this protocol, ΔCq values were calculated: ΔCq = Cq(individual microRNA) – Cq(panel’s average).
Different sample groups were compared by a two-sided unpaired t-test to find statistically significant dysregulated microRNA expressions: 1. patients vs. healthy individuals 2. Refractory patients vs responding patients. For this, the ΔCq values of each microRNA were compared between the formed groups. The fold-change of exosomal microRNA was calculated as follows:
$\text{fold-change}=2^{-(\Delta Cq(group1)-\Delta Cq(group2))}$.

To correct for multiple testing, the Holm-Šídák method was applied to the determined p-values using the Graph pad prism algorithm.

3.2.17 NormFinder

For the NormFinder algorithm, the ΔCq values of all samples (healthy and diseased) were compared to find the most stable expressed microRNAs. Calculated stability values were arranged from stable to highly variating. After exclusion of the exogenous control readout samples, the microRNA with the highest stability value, let-7d, was chosen as housekeeper for single assay normalizations.

3.2.18 qPCR analysis for single miRNA primers

For the analysis of the top candidates from the primary patients focus panel data in PDX sera, 1 ml PDX serum was used as starting material. The serum was precleared by the sequential centrifugation protocol as well as ultracentrifugation. Ultracentrifugation pellets were resolved in 100 µl PBS and incubated with 500 µl immunocapture bead solution. TRIzol isolation was performed as described above, RNA was resuspended in 6,5 µl RNAse-free water.

For reverse transcription, the miRCURY protocol instructions were followed. The maximum RNA input of 6.5 µl, isolated via TRIzol protocol, 2 µl of reaction buffer containing the primers and dNTPs, 1 µl reverse transcriptase as well as 0.5 µl of a synthetic RNA spike-in UniSp6 used to control cDNA synthesis efficiency was pipetted in a RNAse-free microcentrifuge tube and incubated for 60 min on 42°C followed by a heat inactivation for 5 min of 95°C.

qPCR was performed according to manufacturer's standard protocol. The synthesized cDNA was added to the reaction mix diluted 1:10 in RNAse-free water. One 10 µl qPCR reaction consisted of 3 µl diluted template, 1 µl of the primer mix, 5 µl of SYBR green master mix and 1 µl RNAse free water. To minimize pipetting and resulting technical variations, the reaction mix was prepared in a separate microcentrifuge tube without the cDNA samples in a total volume 10% higher than needed. 7 µl of this master mix was transferred to a 96-well light cycler plate for each sample. Finally, 3 µl of diluted cDNA per well was thoroughly mixed in.

The Light cycler was programmed as described above.

4. Results

4.1 Exosomal microRNA expression differs significantly between leukemia patients vs healthy individuals and between therapy refractory vs therapy responding patients

We compared exosomal microRNA expression of pediatric B-ALL patients with different clinical courses and the expression in healthy individuals in order to find expression differences and identify candidate microRNAs to investigate in more detail. Exosomes were isolated by ultracentrifugation from 1.5 ml plasma of pediatric patients suffering from precusor B-ALL, both at the timepoint of diagnosis (n=8, Table 1a) and relapse (n=3, Table 1b), as well as from healthy individuals (n=3).

The exosomal RNA was isolated and measured in a qPCR panel analyzing the expression of 179 different microRNAs. For this, the miRCURY LNA miRNA PCR system, a quantitative polymerase chain reaction (qPCR) system optimized for the amplification of low concentrated microRNAs, was used.

Expression profiles were compared between predetermined clinical groups to select microRNAs capable of distinguishing one group from the other and therefore being candidates suitable for a liquid biopsy:

Patients' samples showed a significantly different expression profile of plasma exosomal microRNA than healthy individuals. In the patients' profile, individual microRNAs were found to be up to 10x higher or lower expressed, compared to the healthy individuals. Various microRNA-expressions reached statistical significance and were therefore identified as candidates to distinguish diseased from healthy individuals (Fig.3a). In unpaired two-sided t-tests, the most significantly upregulated microRNAs in the patients' exosomes were mir-92a-3p, mir-25-3p and mir-484 (Fig.3b). In an adjustment for multiple testing using the Holm-Šídák-method, mir-484 upregulation was significant (p=0.0325). Four candidate microRNAs were present in all leukemia samples but were not amplified in any healthy control sample: mir-505-3p, mir-132-3p, mir-421 and mir-7-1-3p (Fig.3c).

Table 1: B-ALL plasma samples‘ clinical data used in the Focus panels

a.	Diagnosis	Age at Diagnosis	Initial leukocyte count	1. stratification	MRD day 29	MRD day 50	2. stratification	Follow up
Pat1	cALL	2	1.33G/L	Low risk	Negative	Negative	Standard	No relapse until now
Pat2	cALL	6	1.09G/l	Low risk	Negative	Negative	Standard	No relapse until now
Pat3	preB ALL	9	3.66G/l	Low risk	Negative	Negative	Standard	No relapse until now
Pat4	cALL	17	5.6G/l	High risk	Negative	Negative	Standard	No relapse until now
Pat5	cALL	11	8.78G/l	High risk	Negative	Negative	Standard	No relapse until now
Pat6	preB ALL	3	56.3 G/l	High risk	Negative	Negative	Standard	No relapse until now
Pat7	cALL	17	7 G/l	High risk	9*10^-2		Modified high risk	Bone marrow transplantation, no relapse until now
Pat8	cALL	2	7.61G/l	Low risk	8*10^-3	6*10^-3	Modified high risk	Bone marrow transplantation, no relapse until now

b.	Diagnosis	Age at re-	No. of re-	Previous therapy				Follow up

		lapse	lapse		
Pat9	PreB ALL	18	4th	2 bone marrow transplantations, CAR-T-Cell therapy	Multiple following relapses, deceased
Pat10	PreB ALL	21	2nd	bone marrow transplantation, CAR-T-Cell therapy	Deceased
Pat11	PreB ALL	2	2nd	2 bone marrow Transplantations, CAR-T cell therapy	Deceased

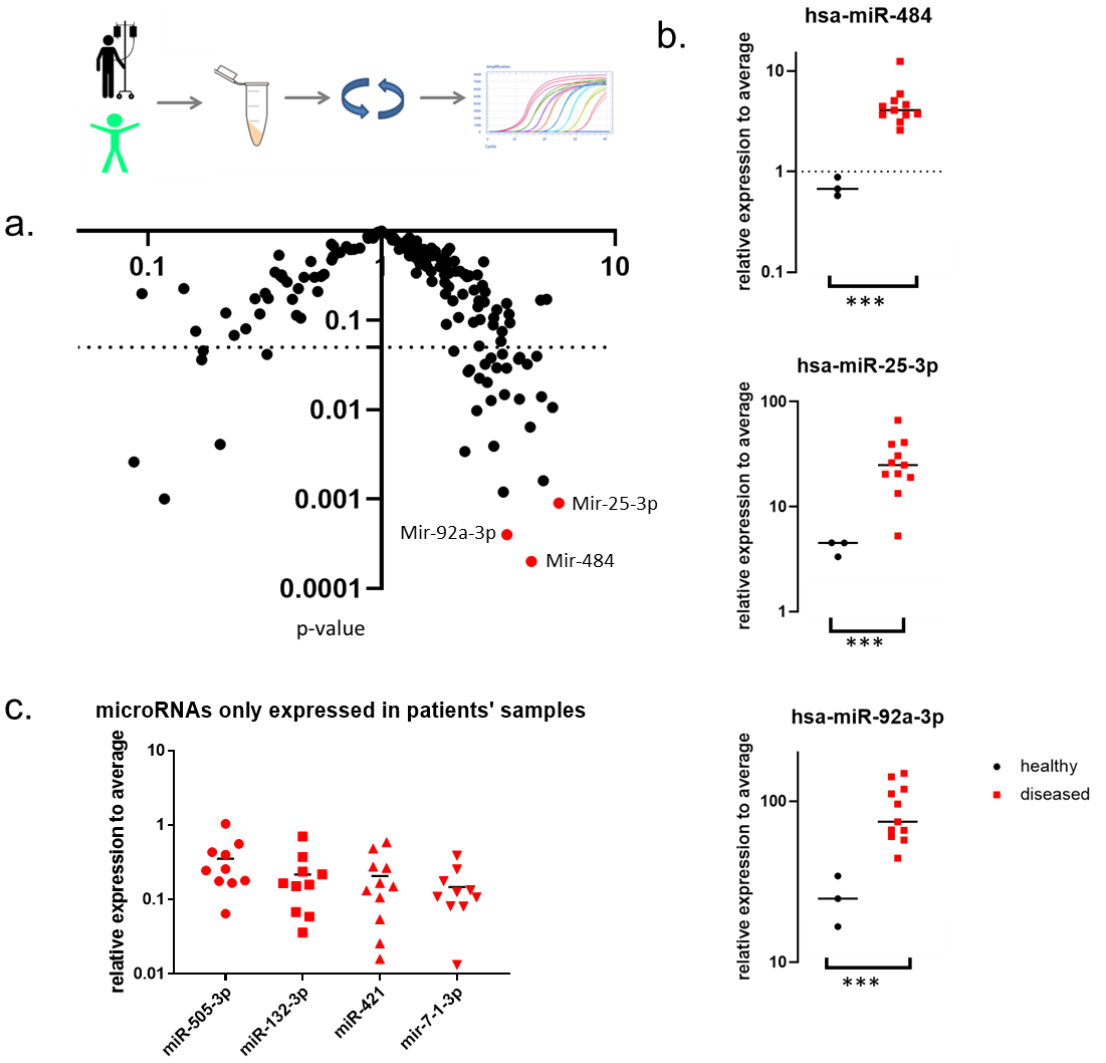

Figure 3: Exosomal microRNA expression in patients vs. healthy controls.
Expression measured by qPCR from RNA isolated from plasma exosomes of precursor B-ALL patients and of healthy individuals.

a. Volcano blot for all analyzed microRNA expressions.
   Fold-change = $2^{-(\text{mean } \Delta Cq(\text{patient})-\text{mean } \Delta Cq(\text{healthy}))}$. Dotted line indicating p=0,05.
b. Three top upregulated microRNAs in leukemia vs healthy. One point depicts one sample's relative expression= $2^{-(\text{mean Cq(target miRNA)-mean Cq (all miRNAs)})}$ of the analyzed microRNA compared to the whole panel's average Cq value.
c. microRNA candidates expressed in all leukemia samples, but in no healthy sample. One point depicts one sample's relative expression= $2^{-(\text{mean Cq(target miRNA)-mean Cq (all miRNAs)})}$ of the analyzed microRNA.

p-value determined by a two-sided unpaired t-test. *** p<0.001

By analyzing the patient group at the timepoint of initial diagnosis in more detail, now dividing it into a therapy refractory (n=2) and therapy responding group (n=6), again microRNA expression differences were found. "Therapy refractory" was defined by the clinical need to modify the standard risk group treatment (see table 1, Pat. 7 and 8).

Though higher p-values were reached in contrast to comparing healthy vs diseased samples, various microRNA expression differences reached statistical significance. Both microRNAs expressed on a higher level in the refractory patients' plasma exosomes, as well as microRNAs expressed on a higher level in responding patients, were found (Fig.4a). Mir-23b-3p and mir-409-3p displayed the most significant upregulation in refractory patients, while mir-7-5p was most significantly downregulated compared to responding patients' plasma exosomes (Fig.4b).

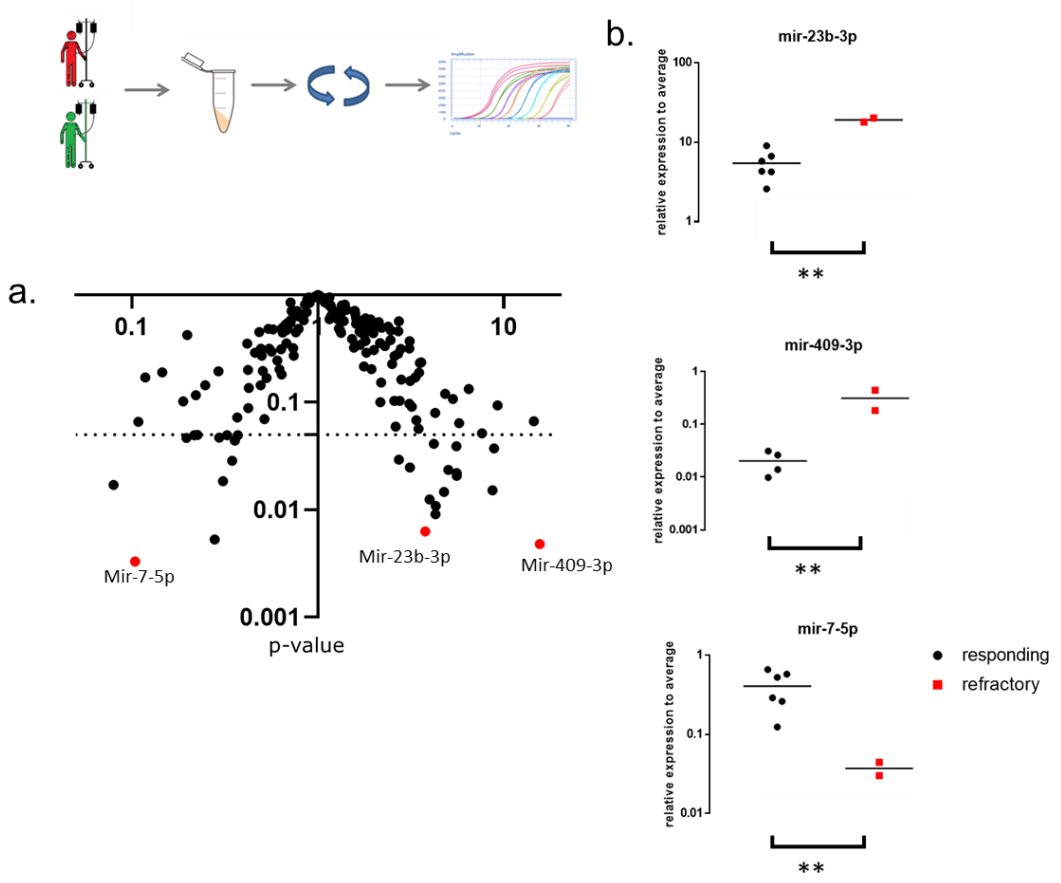

Figure 4: Exosomal microRNA expression in refractory vs responding patients.
Expression measured by qPCR from RNA isolated out of plasma exosomes of precursor B-ALL patients.

a. Volcano blot for all analyzed microRNA expressions.
   Fold-change = $2^{-(\text{mean } \Delta Cq(\text{refractory})-\text{mean } \Delta Cq(\text{responding}))}$. Dotted line indicating p=0,05.
b. Three top dysregulated microRNAs in refractory vs responding. One point depicts one sample's relative expression= $2^{-(\text{mean Cq(target miRNA)-mean Cq (all miRNAs)})}$ of the analyzed microRNA compared to the whole panel's average Cq value.

p-value determined by a two-sided unpaired t-test. **p<0.01

4.2 Establishment of a leukemia-specific exosome isolation method

With the identification of differentially regulated exosomal microRNAs in patients' plasma, strong candidates as biomarkers for liquid biopsy-based approaches have been discovered. Nevertheless, it remains uncertain whether the dysregulated exosomal cargo is secreted by the leukemia cells for niche reprogramming and therefore are functionally relevant, or by bystander cells affected by the changes induced by leukemic cells. For further investigation of the mechanism by which the dysregulated microRNAs could contribute to chemoprotection, it is necessary to confirm the cells of origin. TEX carry no specific surface feature separating them from physiologic exosomes, making it impossible to separate tumor and non-tumor derived exosomes in primary samples. In a mouse xenotransplantation model however, the leukemia is the only human element contributing to circulating exosomes. Therefore, a human specific extraction of exosomes from serum of xenotransplanted mice is tumor specific, and characterization of the extracted exosomes gives insight about the cargo of TEX.

4.2.1 Anti-CD63 clone H5C6 binds to cellular CD63 human-specifically

CD63 is one of the most established exosomal marker proteins, since it is enriched on exosomal membranes [163] and absent in extracellular vesicles in the same size range, namely microvesicles [15]. The amino acid sequence of human and murine CD63 is around 80% identical. With an antibody specifically binding to the human CD63 epitope, but not interacting with the murine CD63+ exosomes, isolation of human-specific exosomes from serum can be achieved.

CD63 is also abundant on the cell membrane [42], which makes it accessible for testing of candidate antibodies for their species-dependent epitope recognition by incubation with cells of human and murine origin.

First species specificity tests were conducted by staining cellular membrane CD63 with anti-CD63 antibodies. Cell lines were chosen to represent the serum exosomes in the PDX-mice: The cell line Nalm6 is derived from human ALL cells, murine peripheral blood mononuclear cells were isolated from blood of control NSG mice.

The anti-CD63 clone H5C6 was found to bind to human CD63, resulting in a strong shift in fluorescent signal compared to the PECy7 isotype control, whereas in the murine peripheral blood cells, no difference in the mean fluorescence intensity was observed.

When staining the cells with the anti-CD63 clone MX95.129.5, both Nalm6 cells and murine peripheral blood cells showed fluorescence in flow cytometry measurement, indicating a cross-reactivity of this anti-CD63 clone to the murine epitope (Fig.5).

Analyzing epitope recognition on murine and human derived cell membrane CD63 identified the antiCD63 clone H5C6 to specifically bind to human CD63.

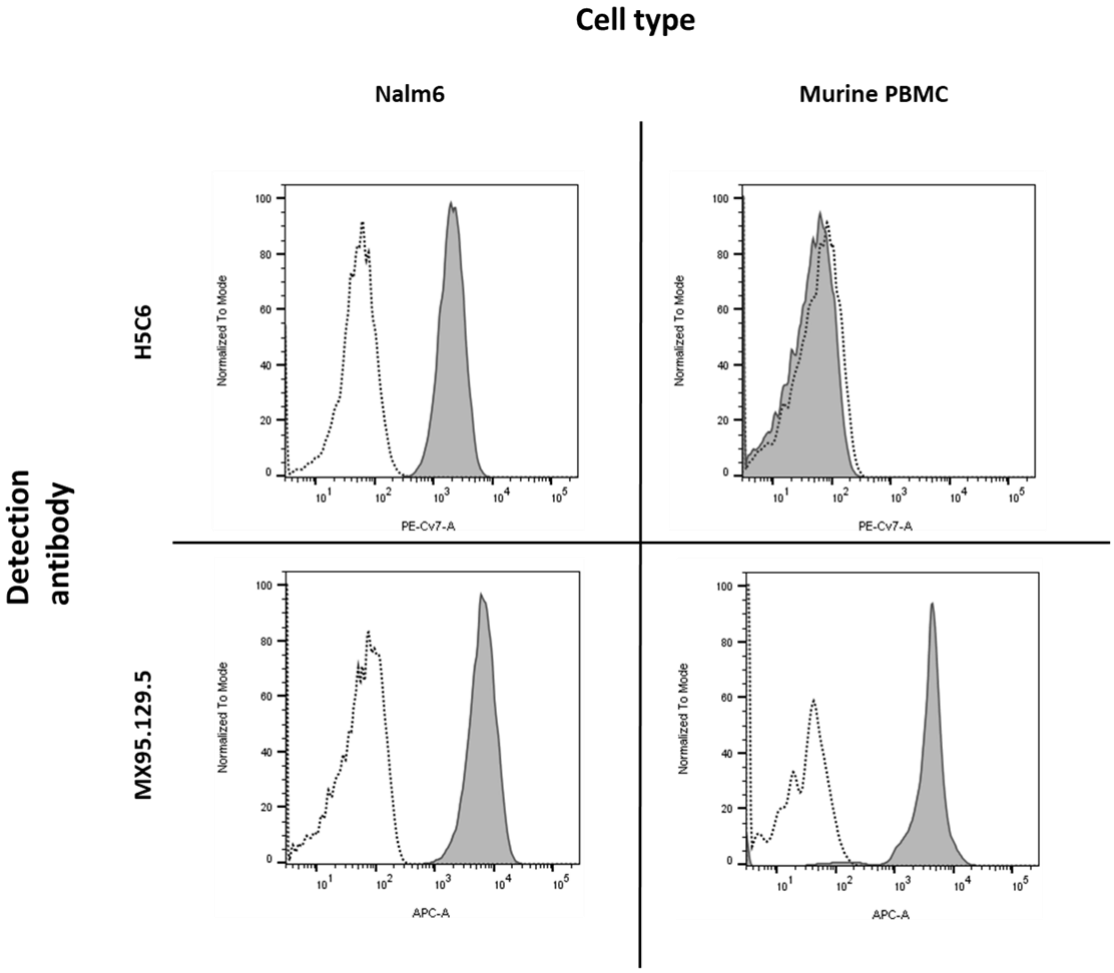

Figure 5: AntiCD63 antibody test on cells.
Staining of surface CD63 on Nalm6 cells and murine peripheral blood mononuclear cells. CD63 signal measured either with the aCD63 antibody H5C6 or the aCD63 antibody MX95.129.5. Dotted histogram: isotype control

4.2.2 Anti-CD63 clone H5C6 binds to exosomal CD63 human-specifically

To validate this finding on exosomal CD63, serum derived exosomes from healthy control serum were stained with the antibodies. With a size range of 40-100 nm, exosomes are too small to be detectable via flow cytometry. To circumvent this, ultracentrifugation enriched exosomes were bound to 4 µm polystyrene beads. The aldehyde group on the beads' surface reacts with proteins' amine groups, forming covalent imide bounds. By binding a purified exosomal fraction unspecifically via surface protein interaction to the beads, no pre-enrichment bias is added to the detection [164]. This way, anti-CD63 antibody candidates can be further validated on their species specificity on exosomes.

Both H5C6 and MX95.129.5 recognized human exosomes bound to the latex beads. For murine samples, the exosomal epitope recognition was significantly increased compared to the control in the MX95.129.5 stained sample, indicating cross-reactivity for murine exosomal CD63, whereas the H5C6 incubated murine sample did not show an increase in fluorescence (Fig.6).

Taking together the antibody tests on cellular and on exosomal level, the data indicates that the anti-CD63 clone H5C6 can recognize and bind to the human CD63 epitope, while not interacting with murine CD63. By covalently coupling this antibody to magnetic beads and incubating serum with them, antibody-bound exosomes can be magnetically pulled down and extracted from the serum. On the other hand, the data indicates recognition of human and murine CD63 for the anti-CD63 clone MX95.129.5, making it an ideal detection antibody to recognize murine contamination in following experiments.

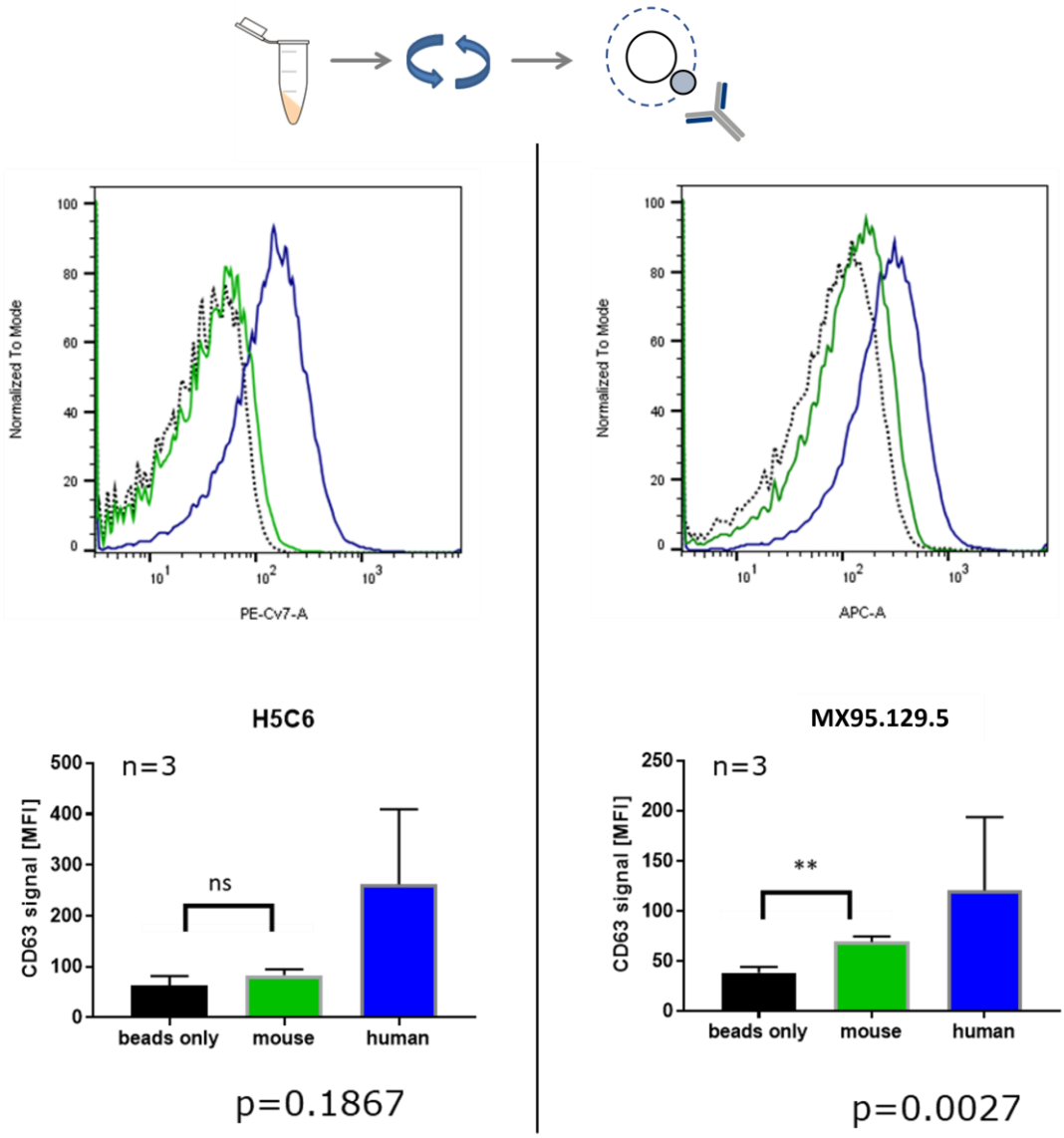

Figure 6: Antibody test on exosomes.
Aldehyde-mediated capture of ultracentrifugation enriched exosomes from different species. CD63 signal measured either by the PE-Cy7 coupled detection antibody H5C6 or the APC coupled detection antibody MX95.129.5. Histogram depicts one representative flow cytometry experiment.
p-value determined by a two-sided unpaired t-test.
**p<0.01

4.2.3 Human exosomes can be isolated from a human to murine serum mixture down to a dilution of 1%

In murine PDX serum, tumor derived human exosomes are mixed with murine non-tumor exosomes as well as various serum components. In an immuno-

magnetic capture assay of this xenograft serum, the H5C6 antibody should specifically extract the human CD63 positive exosomes, since other CD63 positive components are precleared by centrifugation, and CD63 positive murine exosomes are not recognized.

To test this hypothesis and to test the minimum concentration of human exosomes needed for isolation, a titration assay of human control serum in non-human control serum was performed. Different percentages of human serum from 1% to 50% were diluted in either mouse or zebrafish serum in a total volume of 100µl. These dilutions were bound to H5C6 beads overnight and the magnetically isolated bead-exosome complexes analyzed via flow cytometry. Since the anti-CD63 clone MX95.129.5 is shown to cross-react with the murine CD63 epitope, the read out with this antibody visualizes possible cross-reactivity of the capture H5C6 bead complex and would detect unspecifically-bound murine CD63+ particles on the magnetic beads.

The titration of human serum in either murine (Fig.7a) or zebrafish (Fig.7b) serum correlates linearly with the mean fluorescent intensity of the detection antibody. In 100% murine serum, the mean fluorescent intensity of the sample lies below the negative, PBS incubated bead control. In both titration experiment, 1% of human serum is detectable via capture and detection of CD63+ vesicles indicated by a shift of mean fluorescence intensity.

The titration in murine serum shows a human specific capture of CD63+ vesicles with neither non-specific nor cross-reactive binding of murine exosomes, nor inhibition of exosome-bead interaction. Since the detection antibody MX95.129.5 does not recognize the zebrafish CD63 epitope, cross-reactivity of the H5C6 capture antibody cannot be ruled out but is unlikely, since CD63 is less conserved in zebrafish (only 46% identity to human CD63). The correlation indicates the absence of inhibitors in the fish serum for CD63 binding of the capture antibody.

Secondly, the titration shows the capability of the assay to extract even small amounts of human exosomes from a murine sample. This indicates that with even small amounts of tumor-derived exosomes in the PDX sera, a human specific isolation of these exosomes is possible and detectable.

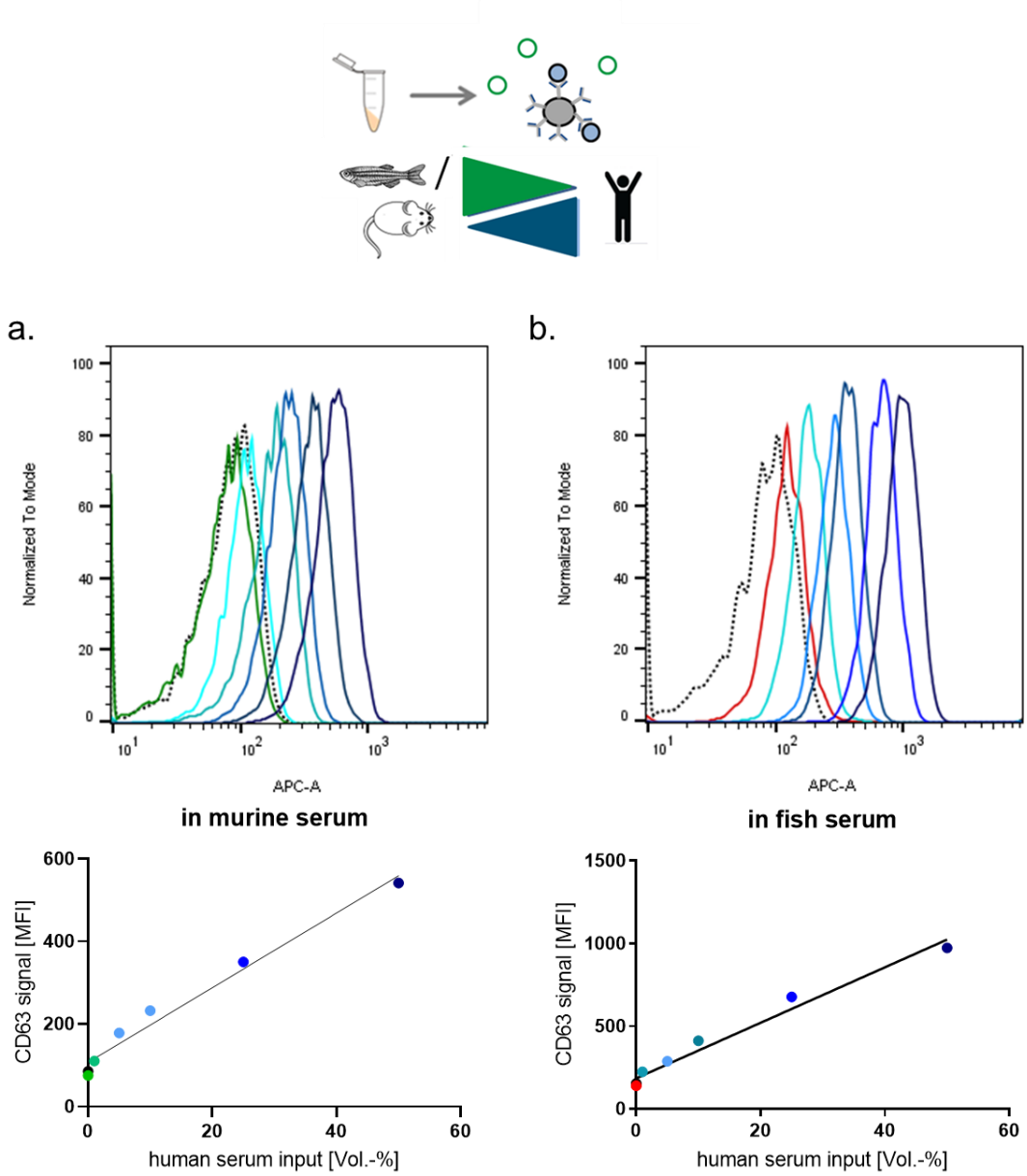

Figure 7: Titration assay.
Immunomagnetic capture via CD63 antibody H5C6 of human exosomes from human control serum titrated in either
a. murine or
b. zebrafish serum.
CD63 signal measured by the mean fluorescence intensity (MFI) of APC coupled to the MX95.129.5 detection antibody.

4.2.4 antiCD63 capture beads isolate leukemia derived exosomes from murine xenograft serum

In the serum of mice engrafted with human leukemia cells, all human exosomes in the mice's blood are leukemia derived mixed with murine components. Apply-

ing the immunocapture assay's capability to isolate exosomes human specifically, all captured exosomes and their cargo from PDX serum will be leukemia derived. This principle has been simulated by the titration assay. To validate the capture of human and therefore leukemia exosomes from PDX serum, immunocaptured PDX serum exosomes from two ALL PDX models and one AML PDX model were tested for exosomal protein markers via FACS.

In all three samples derived from xenografted murine serum, human exosomal markers CD63 and CD81 were present (Fig.8a). The signal strength varied between the samples, correlating to the cellular expression levels of each marker respectively (Fig.8b).

PDX serum contains leukemia/human derived exosomes and murine exosomes. Therefore, the serum can be viewed as a dilution of human exosomes in murine exosomes. Comparing the measured human CD63 fluorescence of the PDX samples to the titration assays line of regression (compare Fig.7), ALL265's mean fluorescence intensity of human exosomes correlated to 0.7% healthy human serum exosomes in murine serum, ALL199's to 9.5% and AML393's to 19.1%.(Fig.8c), illustrating that a considerable percentage of all serum exosomes in PDX mice with advanced leukemia is tumor derived.

This experiment shows the capability of the established immunocapture assay to isolate leukemia derived exosomes in the serum of PDX mice. It indicates that leukemia derived exosomes can make up a significant proportion of circulating exosomes, underlining the possibilities of exosome-mediated tumor influence on patients.

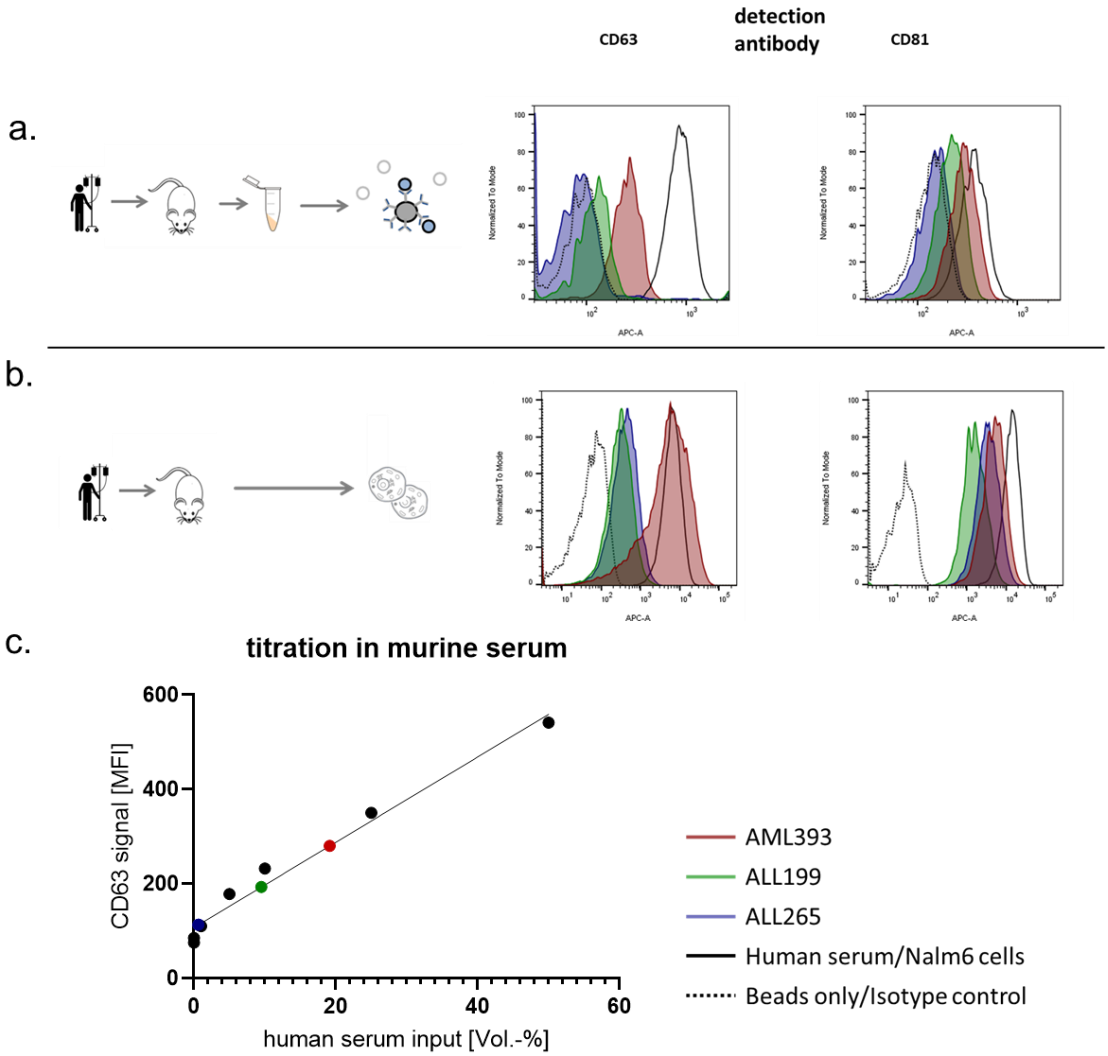

Figure 8: Capture of leukemia-derived exosomes from PDX serum.
Exosome protein marker detection of

a. exosomes from full PDX mice with advanced leukemia, captured via human specific H5C6 antiCD63 binding
b. isolated leukemia cells from PDX mice with advanced leukemia.

CD63 signal measured with the detection antibody MX95.129.5 coupled to APC, CD81 signal measured with the detection antibody JS-81 coupled to APC.

c. Mean fluorescence intensity of the captured PDX serum exosomes‘ CD63 signal correlated to human in murine serum titration according to Figure 7.

4.2.5 Isolated exosomes contain intact exosomal RNA

RNA extraction was performed on all isolated exosome samples via Phenol-chloroform extraction. Because of the high complexity of the starting material and the low concentrations of RNA, quality controls to affirm the exosomal origin of the extracted RNA were performed. The traditional phenol-chloroform extraction of RNA results in an RNA output independent of RNA size, so that both microRNA for expression analysis and mRNA and rRNA for quality control could be recovered.

Due to the specific loading of exosomes, RNA in the size of under 200bp is enriched, whereas the rRNA concentration is low to non-present, resulting in a typical “exosomal” size distribution. The RNA size distribution in the samples was determined by a digital RNA electrophoresis using Agilent Bioanalyzer pico chips after TRIzol RNA isolation. Both in the ultracentrifugation enriched and CD63-isolated exosome samples, the exosomal size distribution was confirmed. Whereas in the ultracentrifuged murine serum exosomal RNA was detectable, it was absent in the immunocapture sample incubated with murine serum, indicating that there was no unspecific carryover of RNA in the workflow and proving the immunocapture assay’s specificity on RNA level (Fig.9a).

To validate the integrity of the extracted exosomal RNA, PCR analysis was used to amplify exosomal mRNAs. *Glyceraldehyde 3-phosphate dehydrogenase (GAPDH)* and *Hypoxanthine-guanine phosphoribosyltransferase (HPRT1)* as well as *C-X-C chemokine receptor type 4 (CXCR4)* mRNA were tested and have been detected in exosomes in literature [159, 160, 165]. In the ultracentrifugation and immunocapture assay, intact mRNA was amplifiable, underlining the isolation of intact exosomal RNA rather than RNA debris. (Fig.9b).

Taken together, this data shows that with our method we were able to extract intact exosomal mRNA from human specific exosomes.

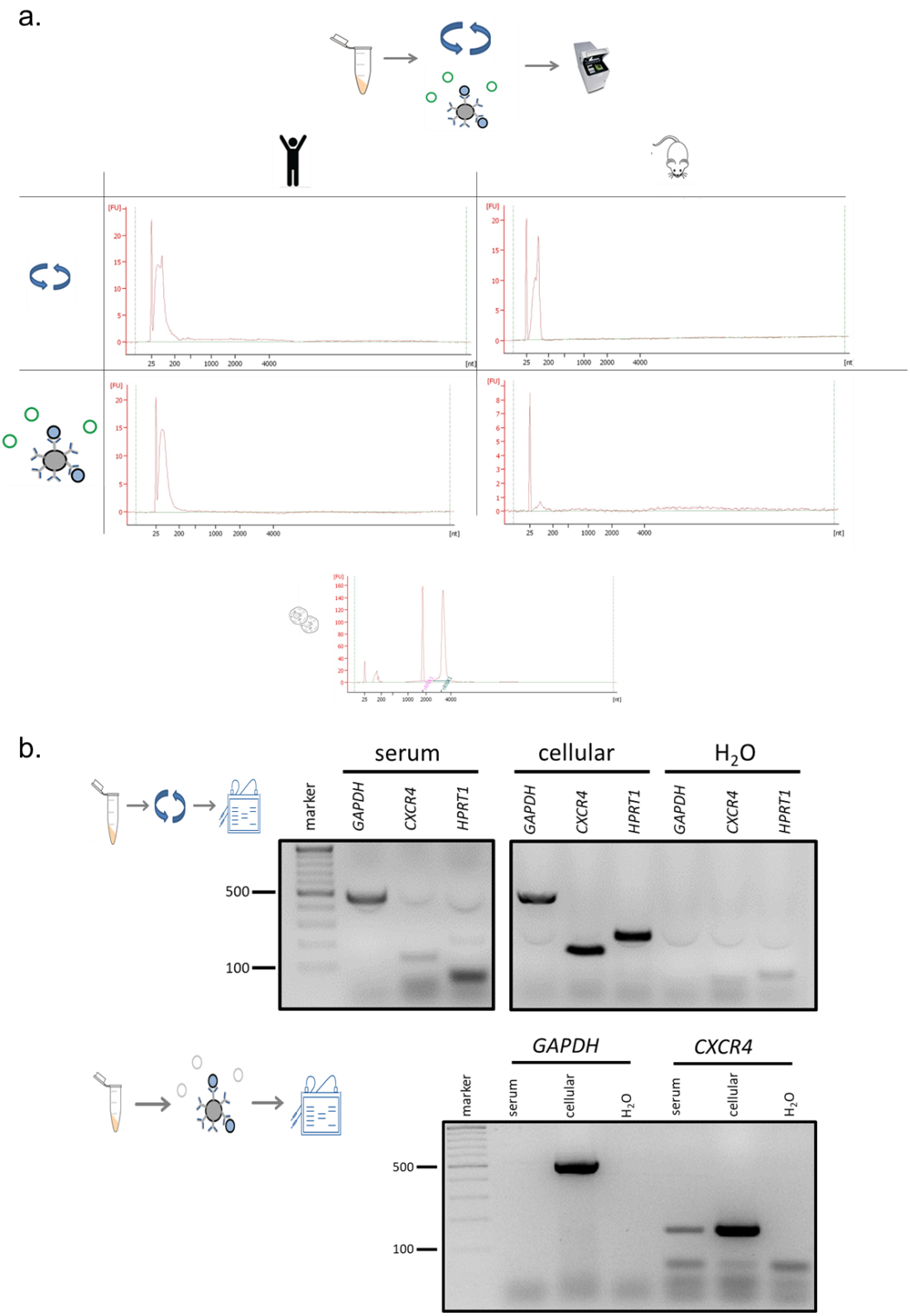

Figure 9: Exosomal RNA extraction and characterization.

a. Bioanalyzer size distribution of extracted RNA of either healthy human or murine serum. Exosomes isolated either by immunocapture or ultracentrifugation. Cellular RNA for comparison.

b. Agarose gel of PCR amplification for exosomal mRNA isolated via immunocapture or ultracentrifugation of healthy human serum.

Cellular RNA extracted from 5 million Nalm6 cells. All RNA extracted via Phenol chloroform extraction.

4.3 Analysis of leukemia derived exosomal microRNAs

We have identified exosomal microRNA dysregulation in the peripheral blood of children suffering from acute B-ALL. Applying the established PDX immunocapture assay, we aimed to not only detect the dysregulation, but also identify the cells of origin for the dysregulated RNAs. For this purpose, first microRNA candidates were chosen from the primary patients' dataset. Then, B-ALL PDX mice were used to isolate leukemia derived exosomal RNA via immunocapture of human exosomes. By amplifying the candidate microRNAs from the leukemia derived exosomal RNA, the leukemia would be proven as the cell of origin for these microRNAs.

4.3.1 Mir-484, mir-25-3p and mir-92a-3p are microRNAs significantly dysregulated in serum exosomes from leukemia patients

To analyze single leukemia derived microRNAs in the PDX mouse model, candidates were chosen from the primary patients' panel data based on differential expression between leukemia and healthy samples, and on their expression level. Data was screened, looking not only for a high fold-change and low p-value in diseased vs. healthy samples, but also for a more abundant expression indicated by a low raw Cq value, making the detection of this microRNA from the low starting concentrations of RNA isolated from the PDX samples more feasible.

Strikingly, the three most significantly upregulated microRNAs, mir-484, mir-25-3p and mir-92a-3p were also found in the top 12 highest dysregulated microRNAs of the panel (Fig.10a). For this reason, they were chosen to be tested in the single kit assays, to answer the question whether the cell of origin is the leukemia cell itself or bystander cells.

In the analysis of single candidate exosomal microRNAs, instead of normalizing to a panel's average microRNA expression, housekeepers must be determined individually for the used material and samples. NormFinder is an algorithm scanning expression panels for the most stable genes. This algorithm was applied to all data of the focus-panel samples, containing both the values of patients and of healthy individuals. Excluding the extrinsic and negative controls, let7d-3p was selected as endogenous microRNA housekeeper for normalization in the single microRNA qPCR assays due to its stable and sufficiently high expression in the primary samples (Fig.10b).

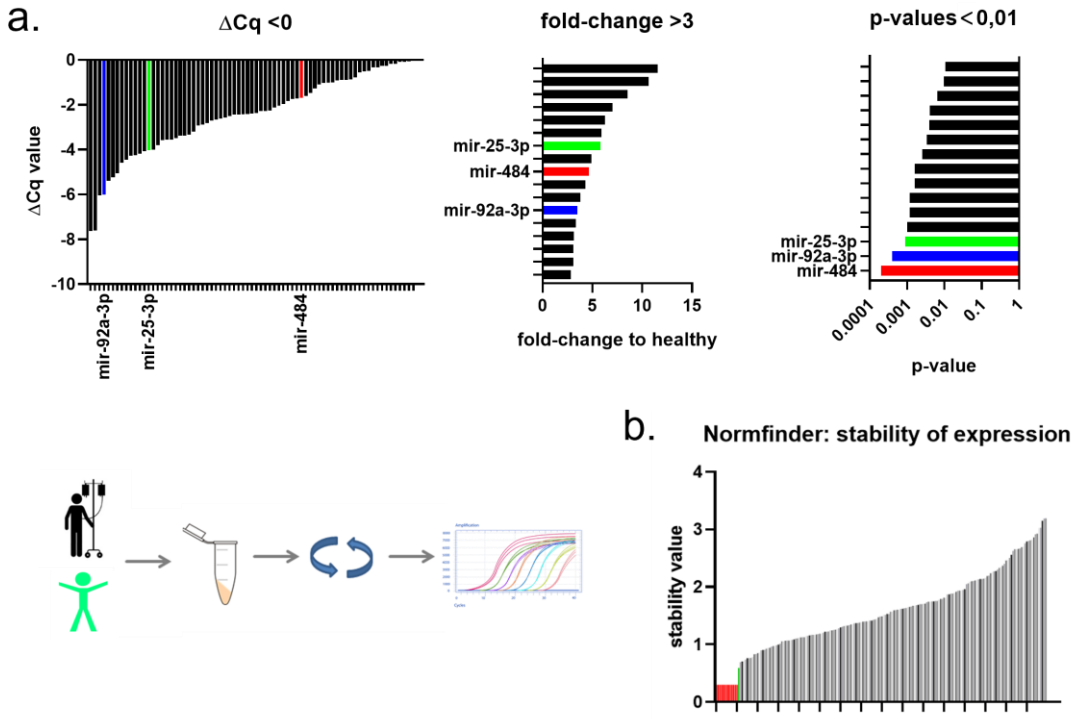

Figure 10: Determination of qPCR single assay candidates.

a. microRNA expression of patients' samples vs healthy controls, three chosen candidate microRNAs highlighted in color (green: mir-25-3p, red: mir-484, blue: mir-92a-3p).
b. NormFinder stability value of all examined microRNAs. Exogenous controls highlighted in red, chosen endogenous normalization microRNA let-7d highlighted in green.

4.3.2 Mir-484, mir-25-3p and mir-92a-3p are detectable in leukemia derived exosomes

Mir-92a-3p, mir-25-3p and mir-484 were picked out as the three top candidates from the primary patients' exosomal microRNA panel. The qPCR data reveals these three microRNAs' potential to serve as biomarkers to distinguish diseased from healthy individuals. To find out whether the leukemic cells are the cells of origin, the expression of the three microRNAs was measured in leukemia derived exosomes from 1 ml PDX serum using the immunocapture assay. As representation of the pediatric ALL patient group, ALL PDX samples from initial diagnosis of pediatric patients (n=2) and relapsed pediatric patients (n=2) were used.

In all four analyzed ALL samples, from initial diagnosis and relapse, leukemia derived exosomes carried mir-92a-3p, mir-25-3p and mir-484. Relative expressions on exosomal and cellular level correlated (Fig.11a). Possibly because of residual murine contamination and since the microRNA primers are not human-specific due to sequence conservation, weak target microRNA expression was also detected in non-injected NSG serum controls. To filter this out, the microRNA levels in PDX samples with advanced leukemia were normalized to the

background signal of non-injected, healthy NSG mice. Here, the lowest expressed microRNA in the non-normalized analysis, mir-484, showed the highest fold-change, indicating an overall low expression of this particular microRNA, but an upregulation in leukemia derived exosomes (Fig.11b).

Although the target microRNAs were chosen based on ALL patients' plasma expression, the analyzed microRNA candidates were also identified as leukemia derived in three AML samples (Fig11a,b).

In summary, this RNA expression analysis combined with the xenograft-immunoassay confirms the leukemic origin of exosomes with differentially expressed mir-92a-3p, mir-25-3p and mir-484. Out of these three, mir-484 shows the strongest leukemia derived difference of expression.

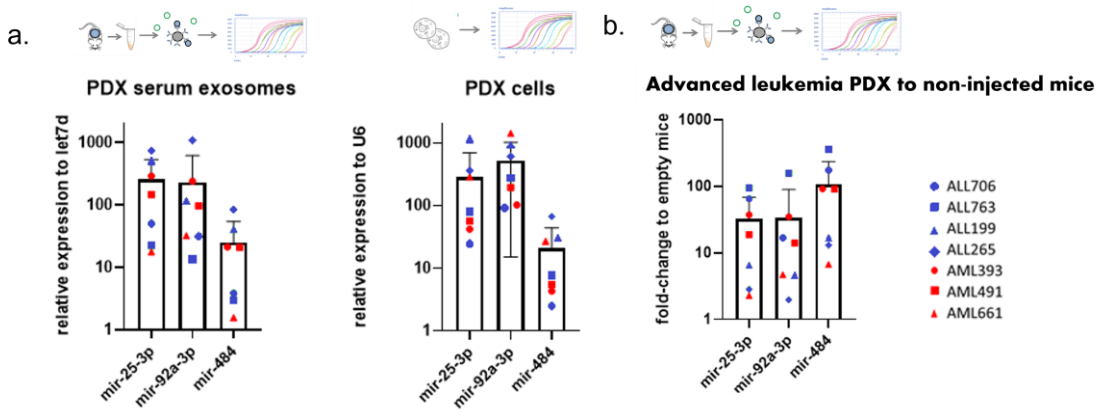

Figure 11: MicroRNA expression in tumor derived exosomes in PDX serum and in PDX cells.

a. Expression of candidate miRNAs in RNA extracted from immunocaptured PDX serum and PDX cells. Relative expression to exogenous control $=2^{-(Cq(target)-Cq(endogenous\ control))}$

b. Expression of candidate miRNAs in RNA extracted from immunocaptured PDX serum compared to non-injected NSG mice serum exosomes.
Fold-change $= 2^{-(\Delta Cq(PDX)-\ \Delta Cq(non\text{-}injected))}$

One point depicts one patient sample analyzed in pooled PDX serum.

5. Discussion

Insights in exosomal functions are more and more applied to the clinical practice in various tumor entities, especially in form of liquid biopsies to improve diagnostic procedures. Nonetheless, diagnostic opportunities making use of exosomes in acute pediatric leukemia currently remain largely untouched.

In our research, we use peripheral blood exosomes to identify biomarker candidates for early detection of therapy refraction in pediatric acute B-cell leukemias. We further developed a novel PDX immunocapture assay to not only identify microRNA expression differences, but to determine the leukemia cells as the cells of origin to allow functional analysis.

Analyzing the data of two refractory and six responding patients' plasma taken at the timepoint of initial diagnosis, we were able to identify a microRNA pattern to pick out the refractory patients as a discovery stage of possible biomarkers.

Upregulation of the two exosomal microRNAs mir-23b-3p and mir-409-3p and a downregulation of mir-7-5p in the refractory samples compared to responding samples were found to indicate the need to intensify therapy after the standard therapy regime due to a lack of complete response. These patterns are found in samples taken at the timepoint of diagnosis, showing that the dysregulation of therapy refractory patients' exosomes is no answer to therapy, but is build up by the leukemia *a priori.*

The found biomarker candidates have been functionally analyzed in cancer exosomes in literature: Ono et al. investigated the exosomal crosstalk between breast cancer cells and the bone marrow niche. In line with our findings, they discovered an upregulation of mir-23b-3p in mesenchymal stem cell derived exosomes. Breast cancer cells treated with these exosomes showed a dormant phenotype and were less susceptible to chemotherapy [166].

In a study of esophageal carcinoma, patients' serum levels of mir-7 prior to therapy correlated with therapy response, affirming our data that low mir-7 concentration predicts poor response to chemotherapy. Interestingly, treatment in this study was radiochemotherapy. Since this therapy resistance cannot be mediated by induction of a direct drug resistance alone, this broader regime compared to single-drug treatment argues in favor of a more complex influence by extracellular mir-7 on the tumor cells , for example introduction of dormancy or increased niche interaction, also protecting the cancer cells from radiation [167].

The found microRNA candidates represent promising therapeutic targets to prevent unfavorable outcome in the future, but studies with a higher case number especially for refractory patients are needed as a verification stage. Since in our data quite recently drawn samples are included, we cannot rule out future late relapses in our responding cohort but focus on the readout of therapy response.

In summary we took the first steps to establish an exosome based liquid biopsy to add to the diagnostic process of pediatric B-ALL. We proof the principle that even at the time of diagnosis, the patients' plasma contains valuable information in the form of exosomes sent out by the leukemia and that this information correlates with clinical outcome.

Whereas in biomarker discovery from primary patients' biofluids no difference is made between TEX and exosomes derived of healthy cells, a new method of isolating and analyzing tumor-derived exosomes is presented in this study., Restricting our PDX immunocapture assay to human CD63+ exosomes out of full-blown leukemia PDX mice, we filter out murine exosomes and are left with information only sent out by the leukemia. By defining the cell of origin, further investigation of the function of the dysregulated exosomal microRNA can be conducted, for example by specific overexpression or labeling of these microRNAs.

It must be considered that this focus on the tumor cells is not necessary for all exosome studies in cancer. New exosomal biomarkers to be used in liquid biopsies can have predictive value no matter the cell of origin. However, potential tumor-derived biomarkers could be diluted out by the bystander-cell exosome signal. This deflection of results is minimized by the species- and tumor-specific analysis.

We present groundwork for the tumor specific isolation of exosomes. In the technical workflow, low concentration and small size of the studied molecules challenge standard protocols. By optimizing these protocols for exosomal dimensions, a downscale to 1 ml of PDX serum as starting material has been achieved for the analysis of leukemia derived exosomal microRNA. Nonetheless, this amount of serum still required pooling serum from multiple mice for one patient sample. The presented method utilizes CD63 as the exosomal marker protein for isolation. A hint that antigen-isolated and size-isolated exosomes consist of different subgroups can be drawn from the isolated exosomal mRNA profiles, in which the CD63+ exosomes showed an enrichment in CXCR4 mRNA. Because CD63 is described as the gold standard of exosomes

markers, this enrichment indicates a precise isolation of exosomes without contamination with other small vesicles.

Since the selection in this assay is human-specific, in principle neither the tumor entity nor the used model is fixed. An application of the tumor-specific immunocapture for different tumor entities is conceivable. PDX models are established for multiple neoplastic diseases, and exosomes from these models have been analyzed [168]. Since leukemia cells are not the only tumor cells to heavily influence their microenvironment, differentiation of tumor derived, and microenvironment derived exosome dysregulations is a crucial information for further insights in these dysregulations in all investigated tumor entities.

The exosome isolation assay is not bound to murine host systems. Depending on the application, specific advantages from other models can be used by transferring the method to it. An experimental setup requiring TEX profiles from individual patients is time consuming in mice, since months can pass between injection and leukemia outbreak. One promising model for faster readout is the zebrafish. Preliminary titration data from our experiments indicate a potential for the use of zebrafish as PDX host, although amounts of serum will be even lower, and methods will have to be adjusted.

Mir-92a-3p, mir-25-3p and mir-484 are significantly upregulated in leukemia samples compared to healthy controls. By applying our new PDX-immunocapture assay, we additionally show that the exosomes containing upregulated mir-92a-3p, mir-25-3p and mir-484 are excreted by leukemia cells rather than bystander cells. Despite its overall low concentration, especially mir-484 is enriched in leukemia derived exosomes. This data indicates specific enrichment processes of these microRNAs from the leukemia cell to the leukemia derived exosomes and suggest the importance of these dysregulations for leukemia progression. Although the candidate microRNAs tested with our PDX-immunocapture assay were chosen from ALL samples, all three exosomal microRNAs have also been identified as leukemia derived in AML samples. This implicates a more general pro-tumor function of exosomal mir-92a-3p, mir-25-3p and mir-484 in acute leukemias.

In various other neoplastic entities, these extracellular microRNAs have been found upregulated compared to healthy individuals, including lung, colorectal, pancreatic and breast cancer for mir-484 [169-172], cervical, colorectal, gastric and breast cancer for mir-92a-3p [173-176] and pancreatic, thyroid cancer as well as osteosarcoma for mir-25-3p [177-179].

In pancreatic cancer, as discovered by Yang et al., high cellular mir-484 is essential for tumorigenesis [180]. Assuming this mechanism for ALL, mir-484 could be transferred from leukemia cell to leukemia cell by exosome as a mechanism of “phenocopying”. Opposed to this finding, low intracellular mir-484 levels are correlated to pro-survival pathways in CLL [181]. If one postulates a similar correlation in ALL, enrichment of mir-484 in leukemia derived exosomes can be interpreted as shuttling-out of adverse microRNA. Arguments for leukemia-bystander cell crosstalk in form of immune cell exhaustion can be deducted from a study by Jieke et al.: Exosomes from both AML and ALL cell lines overexpressing mir-92a-3p impair function and induce apoptosis of T-cells *in vivo* [182].

In summary, we verify the leukemia cells as the cells of origin for the differently expressed microRNAs with the leukemia specific immunocapture assay. By determining the cell of origin, further functional studies are made possible. Although reasonable hypothesizes for the function of these expression differences can be deducted from literature, the interaction of microRNAs and their numerous targets is highly complex and is shown to differ between diseases. Our study presents highly interesting microRNA targets for further studies of their mechanisms in ALL and their role in leukemia derived communication. Investigating the reason for the differential expression of leukemia derived exosomal microRNA is one important step to discover therapeutic chances targeting leukemia communication, for example with the use of antisense microRNAs, therapeutic exosome application or exosome depletion.

References

1. Moricke, A., et al., *Long-term results of five consecutive trials in childhood acute lymphoblastic leukemia performed by the ALL-BFM study group from 1981 to 2000.* Leukemia, 2010. **24**(2): p. 265-84.
2. Schrappe, M., et al., *Outcomes after induction failure in childhood acute lymphoblastic leukemia.* N Engl J Med, 2012. **366**(15): p. 1371-81.
3. Oskarsson, T., et al., *Relapsed childhood acute lymphoblastic leukemia in the Nordic countries: prognostic factors, treatment and outcome.* Haematologica, 2016. **101**(1): p. 68-76.
4. Nagpal, M., et al., *Tumor markers: A diagnostic tool.* National journal of maxillofacial surgery, 2016. **7**(1): p. 17-20.
5. Hong, Y. and Q. Zhang, *Phenotype of circulating tumor cell: face-off between epithelial and mesenchymal masks.* Tumour Biol, 2016. **37**(5): p. 5663-74.
6. Cabel, L., et al., *Circulating tumor cells: clinical validity and utility.* Int J Clin Oncol, 2017. **22**(3): p. 421-430.
7. Heitzer, E., P. Ulz, and J.B. Geigl, *Circulating tumor DNA as a liquid biopsy for cancer.* Clin Chem, 2015. **61**(1): p. 112-23.
8. Jahr, S., et al., *DNA fragments in the blood plasma of cancer patients: quantitations and evidence for their origin from apoptotic and necrotic cells.* Cancer Res, 2001. **61**(4): p. 1659-65.
9. Garcia-Olmo, D.C., et al., *Cell-free nucleic acids circulating in the plasma of colorectal cancer patients induce the oncogenic transformation of susceptible cultured cells.* Cancer Res, 2010. **70**(2): p. 560-7.
10. Breveglieri, G., et al., *Non-invasive Prenatal Testing Using Fetal DNA.* Mol Diagn Ther, 2019. **23**(2): p. 291-299.
11. Cheng, L., et al., *Exosomes provide a protective and enriched source of miRNA for biomarker profiling compared to intracellular and cell-free blood.* J Extracell Vesicles, 2014. **3**.
12. Caby, M.P., et al., *Exosomal-like vesicles are present in human blood plasma.* Int Immunol, 2005. **17**(7): p. 879-87.
13. Hoshino, A., et al., *Tumour exosome integrins determine organotropic metastasis.* Nature, 2015. **527**(7578): p. 329-35.
14. Johnstone, R.M., et al., *Vesicle formation during reticulocyte maturation. Association of plasma membrane activities with released vesicles (exosomes).* J Biol Chem, 1987. **262**(19): p. 9412-20.
15. Kowal, J., et al., *Proteomic comparison defines novel markers to characterize heterogeneous populations of extracellular vesicle subtypes.* Proc Natl Acad Sci U S A, 2016. **113**(8): p. E968-77.
16. Heijnen, H.F., et al., *Activated platelets release two types of membrane vesicles: microvesicles by surface shedding and exosomes derived from exocytosis of multivesicular bodies and alpha-granules.* Blood, 1999. **94**(11): p. 3791-9.
17. Stoorvogel, W., et al., *Late endosomes derive from early endosomes by maturation.* Cell, 1991. **65**(3): p. 417-27.
18. Sotelo, J.R. and K.R. Porter, *An electron microscope study of the rat ovum.* J Biophys Biochem Cytol, 1959. **5**(2): p. 327-42.

19. Stuffers, S., et al., *Multivesicular endosome biogenesis in the absence of ESCRTs.* Traffic, 2009. **10**(7): p. 925-37.

20. Trajkovic, K., et al., *Ceramide triggers budding of exosome vesicles into multivesicular endosomes.* Science, 2008. **319**(5867): p. 1244-7.

21. Mobius, W., et al., *Recycling compartments and the internal vesicles of multivesicular bodies harbor most of the cholesterol found in the endocytic pathway.* Traffic, 2003. **4**(4): p. 222-31.

22. Hurwitz, S.N., et al., *Nanoparticle analysis sheds budding insights into genetic drivers of extracellular vesicle biogenesis.* J Extracell Vesicles, 2016. **5**: p. 31295.

23. Maas, S.L.N., X.O. Breakefield, and A.M. Weaver, *Extracellular Vesicles: Unique Intercellular Delivery Vehicles.* Trends Cell Biol, 2017. **27**(3): p. 172-188.

24. Silva, M. and S.A. Melo, *Non-coding RNAs in Exosomes: New Players in Cancer Biology.* Curr Genomics, 2015. **16**(5): p. 295-303.

25. Kajimoto, T., et al., *Ongoing activation of sphingosine 1-phosphate receptors mediates maturation of exosomal multivesicular endosomes.* Nat Commun, 2013. **4**: p. 2712.

26. Crescitelli, R., et al., *Distinct RNA profiles in subpopulations of extracellular vesicles: apoptotic bodies, microvesicles and exosomes.* J Extracell Vesicles, 2013. **2**.

27. Nolte-'t Hoen, E.N., et al., *Deep sequencing of RNA from immune cell-derived vesicles uncovers the selective incorporation of small non-coding RNA biotypes with potential regulatory functions.* Nucleic Acids Res, 2012. **40**(18): p. 9272-85.

28. Batagov, A.O. and I.V. Kurochkin, *Exosomes secreted by human cells transport largely mRNA fragments that are enriched in the 3'-untranslated regions.* Biol Direct, 2013. **8**: p. 12.

29. Bolukbasi, M.F., et al., *miR-1289 and "Zipcode"-like Sequence Enrich mRNAs in Microvesicles.* Mol Ther Nucleic Acids, 2012. **1**: p. e10.

30. de Jong, O.G., et al., *Cellular stress conditions are reflected in the protein and RNA content of endothelial cell-derived exosomes.* J Extracell Vesicles, 2012. **1**.

31. Wightman, B., I. Ha, and G. Ruvkun, *Posttranscriptional regulation of the heterochronic gene lin-14 by lin-4 mediates temporal pattern formation in C. elegans.* Cell, 1993. **75**(5): p. 855-62.

32. Lee, Y., et al., *MicroRNA maturation: stepwise processing and subcellular localization.* Embo j, 2002. **21**(17): p. 4663-70.

33. Lee, Y., et al., *The nuclear RNase III Drosha initiates microRNA processing.* Nature, 2003. **425**(6956): p. 415-9.

34. Denli, A.M., et al., *Processing of primary microRNAs by the Microprocessor complex.* Nature, 2004. **432**(7014): p. 231-5.

35. Ying, S.Y. and S.L. Lin, *Intron-mediated RNA interference and microRNA biogenesis.* Methods Mol Biol, 2009. **487**: p. 387-413.

36. Bohnsack, M.T., K. Czaplinski, and D. Gorlich, *Exportin 5 is a RanGTP-dependent dsRNA-binding protein that mediates nuclear export of pre-miRNAs.* Rna, 2004. **10**(2): p. 185-91.

37. Hutvagner, G., et al., *A cellular function for the RNA-interference enzyme Dicer in the maturation of the let-7 small temporal RNA.* Science, 2001. **293**(5531): p. 834-8.

38. Villarroya-Beltri, C., et al., *Sumoylated hnRNPA2B1 controls the sorting of miRNAs into exosomes through binding to specific motifs.* Nat Commun, 2013. **4**: p. 2980.

39. Koppers-Lalic, D., et al., *Nontemplated nucleotide additions distinguish the small RNA composition in cells from exosomes.* Cell Rep, 2014. **8**(6): p. 1649-1658.

40. Gibbings, D.J., et al., *Multivesicular bodies associate with components of miRNA effector complexes and modulate miRNA activity.* Nat Cell Biol, 2009. **11**(9): p. 1143-9.

41. Guduric-Fuchs, J., et al., *Selective extracellular vesicle-mediated export of an overlapping set of microRNAs from multiple cell types.* BMC Genomics, 2012. **13**: p. 357.

42. Pols, M.S. and J. Klumperman, *Trafficking and function of the tetraspanin CD63.* Exp Cell Res, 2009. **315**(9): p. 1584-92.

43. Escola, J.M., et al., *Selective enrichment of tetraspan proteins on the internal vesicles of multivesicular endosomes and on exosomes secreted by human B-lymphocytes.* J Biol Chem, 1998. **273**(32): p. 20121-7.

44. Valadi, H., et al., *Exosome-mediated transfer of mRNAs and microRNAs is a novel mechanism of genetic exchange between cells.* Nat Cell Biol, 2007. **9**(6): p. 654-9.

45. Wu, C.X. and Z.F. Liu, *Proteomic Profiling of Sweat Exosome Suggests its Involvement in Skin Immunity.* J Invest Dermatol, 2018. **138**(1): p. 89-97.

46. Zheng, X., et al., *Exosome analysis: a promising biomarker system with special attention to saliva.* J Membr Biol, 2014. **247**(11): p. 1129-36.

47. Gui, Y., et al., *Altered microRNA profiles in cerebrospinal fluid exosome in Parkinson disease and Alzheimer disease.* Oncotarget, 2015. **6**(35): p. 37043-53.

48. Rand, M.L., et al., *Rapid clearance of procoagulant platelet-derived microparticles from the circulation of rabbits.* J Thromb Haemost, 2006. **4**(7): p. 1621-3.

49. Takahashi, Y., et al., *Visualization and in vivo tracking of the exosomes of murine melanoma B16-BL6 cells in mice after intravenous injection.* J Biotechnol, 2013. **165**(2): p. 77-84.

50. Ge, Q., et al., *miRNA in plasma exosome is stable under different storage conditions.* Molecules, 2014. **19**(2): p. 1568-75.

51. Tian, T., et al., *Exosome uptake through clathrin-mediated endocytosis and macropinocytosis and mediating miR-21 delivery.* J Biol Chem, 2014. **289**(32): p. 22258-67.

52. Christianson, H.C., et al., *Cancer cell exosomes depend on cell-surface heparan sulfate proteoglycans for their internalization and functional activity.* Proc Natl Acad Sci U S A, 2013. **110**(43): p. 17380-5.

53. Clayton, A., et al., *Adhesion and signaling by B cell-derived exosomes: the role of integrins.* Faseb j, 2004. **18**(9): p. 977-9.

54. Calzolari, A., et al., *TfR2 localizes in lipid raft domains and is released in exosomes to activate signal transduction along the MAPK pathway.* J Cell Sci, 2006. **119**(Pt 21): p. 4486-98.

55. Lugini, L., et al., *Immune surveillance properties of human NK cell-derived exosomes.* J Immunol, 2012. **189**(6): p. 2833-42.

56. Wang, G.J., et al., *Thymus exosomes-like particles induce regulatory T cells.* J Immunol, 2008. **181**(8): p. 5242-8.

57. Lai, C.P., et al., *Visualization and tracking of tumour extracellular vesicle delivery and RNA translation using multiplexed reporters.* Nat Commun, 2015. **6**: p. 7029.

58. van Balkom, B.W., et al., *Endothelial cells require miR-214 to secrete exosomes that suppress senescence and induce angiogenesis in human and mouse endothelial cells.* Blood, 2013. **121**(19): p. 3997-4006, s1-15.

59. Kogure, T., et al., *Intercellular nanovesicle-mediated microRNA transfer: a mechanism of environmental modulation of hepatocellular cancer cell growth.* Hepatology, 2011. **54**(4): p. 1237-48.

60. Hammond, S.M., et al., *Argonaute2, a link between genetic and biochemical analyses of RNAi.* Science, 2001. **293**(5532): p. 1146-50.

61. Gu, S., et al., *Biological basis for restriction of microRNA targets to the 3' untranslated region in mammalian mRNAs.* Nat Struct Mol Biol, 2009. **16**(2): p. 144-50.

62. Baek, D., et al., *The impact of microRNAs on protein output.* Nature, 2008. **455**(7209): p. 64-71.

63. Liu, J., et al., *Argonaute2 is the catalytic engine of mammalian RNAi.* Science, 2004. **305**(5689): p. 1437-41.

64. Rehwinkel, J., et al., *A crucial role for GW182 and the DCP1:DCP2 decapping complex in miRNA-mediated gene silencing.* Rna, 2005. **11**(11): p. 1640-7.

65. Fabbri, M., et al., *MicroRNAs bind to Toll-like receptors to induce prometastatic inflammatory response.* Proc Natl Acad Sci U S A, 2012. **109**(31): p. E2110-6.

66. Royo, F., et al., *Transcriptome of extracellular vesicles released by hepatocytes.* PLoS One, 2013. **8**(7): p. e68693.

67. Goldie, B.J., et al., *Activity-associated miRNA are packaged in Map1b-enriched exosomes released from depolarized neurons.* Nucleic Acids Res, 2014. **42**(14): p. 9195-208.

68. Hayashi, T., et al., *Exosomal MicroRNA Transport from Salivary Mesenchyme Regulates Epithelial Progenitor Expansion during Organogenesis.* Dev Cell, 2017. **40**(1): p. 95-103.

69. Hong, C.S., et al., *Plasma exosomes as markers of therapeutic response in patients with acute myeloid leukemia.* Front Immunol, 2014. **5**: p. 160.

70. De Luca, L., et al., *Characterization and prognostic relevance of circulating microvesicles in chronic lymphocytic leukemia.* Leukemia & Lymphoma, 2017. **58**(6): p. 1424-1432.

71. Marleau, A.M., et al., *Exosome removal as a therapeutic adjuvant in cancer.* J Transl Med, 2012. **10**: p. 134.

72. Pando, A., et al., *Extracellular vesicles in leukemia.* Leuk Res, 2018. **64**: p. 52-60.

73. Chen, W.X., et al., *Exosomes from drug-resistant breast cancer cells transmit chemoresistance by a horizontal transfer of microRNAs.* PLoS One, 2014. **9**(4): p. e95240.

74. Zomer, A., et al., *In Vivo imaging reveals extracellular vesicle-mediated phenocopying of metastatic behavior.* Cell, 2015. **161**(5): p. 1046-1057.

75. Khan, S., et al., *Extracellular, cell-permeable survivin inhibits apoptosis while promoting proliferative and metastatic potential.* Br J Cancer, 2009. **100**(7): p. 1073-86.

76. Le, M.T., et al., *miR-200-containing extracellular vesicles promote breast cancer cell metastasis.* J Clin Invest, 2014. **124**(12): p. 5109-28.

77. Al-Nedawi, K., et al., *Intercellular transfer of the oncogenic receptor EGFRvIII by microvesicles derived from tumour cells.* Nat Cell Biol, 2008. **10**(5): p. 619-24.

78. Corcoran, C., et al., *Docetaxel-resistance in prostate cancer: evaluating associated phenotypic changes and potential for resistance transfer via exosomes.* PLoS One, 2012. **7**(12): p. e50999.

79. Shedden, K., et al., *Expulsion of small molecules in vesicles shed by cancer cells: association with gene expression and chemosensitivity profiles.* Cancer Res, 2003. **63**(15): p. 4331-7.

80. Aung, T., et al., *Exosomal evasion of humoral immunotherapy in aggressive B-cell lymphoma modulated by ATP-binding cassette transporter A3.* Proc Natl Acad Sci U S A, 2011. **108**(37): p. 15336-41.

81. Ciravolo, V., et al., *Potential role of HER2-overexpressing exosomes in countering trastuzumab-based therapy.* J Cell Physiol, 2012. **227**(2): p. 658-67.

82. Taylor, D.D., et al., *T-cell apoptosis and suppression of T-cell receptor/CD3-zeta by Fas ligand-containing membrane vesicles shed from ovarian tumors.* Clin Cancer Res, 2003. **9**(14): p. 5113-9.

83. Wieckowski, E.U., et al., *Tumor-derived microvesicles promote regulatory T cell expansion and induce apoptosis in tumor-reactive activated CD8+ T lymphocytes.* J Immunol, 2009. **183**(6): p. 3720-30.

84. Bergmann, C., et al., *Tumor-derived microvesicles in sera of patients with head and neck cancer and their role in tumor progression.* Head Neck, 2009. **31**(3): p. 371-80.

85. Clayton, A., et al., *Human tumor-derived exosomes selectively impair lymphocyte responses to interleukin-2.* Cancer Res, 2007. **67**(15): p. 7458-66.

86. Szajnik, M., et al., *Tumor-derived microvesicles induce, expand and up-regulate biological activities of human regulatory T cells (Treg).* PLoS One, 2010. **5**(7): p. e11469.

87. Szczepanski, M.J., et al., *Increased frequency and suppression by regulatory T cells in patients with acute myelogenous leukemia.* Clin Cancer Res, 2009. **15**(10): p. 3325-32.

88. Clayton, A., et al., *Human tumor-derived exosomes down-modulate NKG2D expression.* J Immunol, 2008. **180**(11): p. 7249-58.

89. Szczepanski, M.J., et al., *Blast-derived microvesicles in sera from patients with acute myeloid leukemia suppress natural killer cell function via membrane-associated transforming growth factor-beta1.* Haematologica, 2011. **96**(9): p. 1302-9.

90. Cooks, T., et al., *Mutant p53 cancers reprogram macrophages to tumor supporting macrophages via exosomal miR-1246.* Nat Commun, 2018. **9**(1): p. 771.

91. Takano, Y., et al., *Circulating exosomal microRNA-203 is associated with metastasis possibly via inducing tumor-associated macrophages in colorectal cancer.* Oncotarget, 2017. **8**(45): p. 78598-78613.

92. Hanahan, D. and R.A. Weinberg, *The hallmarks of cancer.* Cell, 2000. **100**(1): p. 57-70.

93. Park, J.E., et al., *Hypoxic tumor cell modulates its microenvironment to enhance angiogenic and metastatic potential by secretion of proteins and exosomes.* Mol Cell Proteomics, 2010. **9**(6): p. 1085-99.

94. Mao, G., et al., *Tumor-derived microRNA-494 promotes angiogenesis in non-small cell lung cancer.* Angiogenesis, 2015. **18**(3): p. 373-82.

95. Al-Nedawi, K., et al., *Endothelial expression of autocrine VEGF upon the uptake of tumor-derived microvesicles containing oncogenic EGFR.* Proc Natl Acad Sci U S A, 2009. **106**(10): p. 3794-9.

96. Vong, S. and R. Kalluri, *The role of stromal myofibroblast and extracellular matrix in tumor angiogenesis.* Genes Cancer, 2011. **2**(12): p. 1139-45.

97. Webber, J., et al., *Cancer exosomes trigger fibroblast to myofibroblast differentiation.* Cancer Res, 2010. **70**(23): p. 9621-30.

98. Gesierich, S., et al., *Systemic induction of the angiogenesis switch by the tetraspanin D6.1A/CO-029.* Cancer Res, 2006. **66**(14): p. 7083-94.

99. Josson, S., et al., *Stromal fibroblast-derived miR-409 promotes epithelial-to-mesenchymal transition and prostate tumorigenesis.* Oncogene, 2015. **34**(21): p. 2690-9.

100. Yang, M., et al., *Microvesicles secreted by macrophages shuttle invasion-potentiating microRNAs into breast cancer cells.* Mol Cancer, 2011. **10**: p. 117.

101. Ostenfeld, M.S., et al., *Cellular disposal of miR23b by RAB27-dependent exosome release is linked to acquisition of metastatic properties.* Cancer Res, 2014. **74**(20): p. 5758-71.

102. Grange, C., et al., *Microvesicles released from human renal cancer stem cells stimulate angiogenesis and formation of lung premetastatic niche.* Cancer Res, 2011. **71**(15): p. 5346-56.

103. Hood, J.L., R.S. San, and S.A. Wickline, *Exosomes released by melanoma cells prepare sentinel lymph nodes for tumor metastasis.* Cancer Res, 2011. **71**(11): p. 3792-801.

104. Rana, S., K. Malinowska, and M. Zoller, *Exosomal tumor microRNA modulates premetastatic organ cells.* Neoplasia, 2013. **15**(3): p. 281-95.

105. Fong, M.Y., et al., *Breast-cancer-secreted miR-122 reprograms glucose metabolism in premetastatic niche to promote metastasis.* Nat Cell Biol, 2015. **17**(2): p. 183-94.

106. Jung, T., et al., *CD44v6 dependence of premetastatic niche preparation by exosomes.* Neoplasia, 2009. **11**(10): p. 1093-105.

107. Abd Elmageed, Z.Y., et al., *Neoplastic reprogramming of patient-derived adipose stem cells by prostate cancer cell-associated exosomes.* Stem Cells, 2014. **32**(4): p. 983-97.

108. Zhu, X., et al., *BCR-ABL1-positive microvesicles transform normal hematopoietic transplants through genomic instability: implications for donor cell leukemia.* Leukemia, 2014. **28**(8): p. 1666-75.

109. Serrano, M., et al., *Oncogenic ras provokes premature cell senescence associated with accumulation of p53 and p16INK4a.* Cell, 1997. **88**(5): p. 593-602.

110. Lee, T.H., et al., *Barriers to horizontal cell transformation by extracellular vesicles containing oncogenic H-ras.* Oncotarget, 2016. **7**(32): p. 51991-52002.

111. Burger, J.A., *Nurture versus nature: the microenvironment in chronic lymphocytic leukemia.* Hematology Am Soc Hematol Educ Program, 2011. **2011**: p. 96-103.

112. Snyder, R., *The bone marrow niche, stem cells, and leukemia: impact of drugs, chemicals, and the environment.* Ann N Y Acad Sci, 2014. **1310**: p. 1-6.

113. Lane, S.W., D.T. Scadden, and D.G. Gilliland, *The leukemic stem cell niche: current concepts and therapeutic opportunities.* Blood, 2009. **114**(6): p. 1150-7.

114. Kumagai, M., et al., *Stroma-supported culture in childhood B-lineage acute lymphoblastic leukemia cells predicts treatment outcome.* J Clin Invest, 1996. **97**(3): p. 755-60.

115. Guerrouahen, B.S., I. Al-Hijji, and A.R. Tabrizi, *Osteoblastic and vascular endothelial niches, their control on normal hematopoietic stem cells, and their consequences on the development of leukemia.* Stem Cells Int, 2011. **2011**: p. 375857.

116. Ishikawa, F., et al., *Chemotherapy-resistant human AML stem cells home to and engraft within the bone-marrow endosteal region.* Nat Biotechnol, 2007. **25**(11): p. 1315-21.

117. Hawkins, E.D., et al., *T-cell acute leukaemia exhibits dynamic interactions with bone marrow microenvironments.* Nature, 2016. **538**(7626): p. 518-522.

118. Sipkins, D.A., et al., *In vivo imaging of specialized bone marrow endothelial microdomains for tumour engraftment.* Nature, 2005. **435**(7044): p. 969-73.

119. Duan, C.W., et al., *Leukemia propagating cells rebuild an evolving niche in response to therapy.* Cancer Cell, 2014. **25**(6): p. 778-93.

120. Manabe, A., et al., *Bone marrow-derived stromal cells prevent apoptotic cell death in B-lineage acute lymphoblastic leukemia.* Blood, 1992. **79**(9): p. 2370-7.

121. Nwabo Kamdje, A.H., et al., *Notch-3 and Notch-4 signaling rescue from apoptosis human B-ALL cells in contact with human bone marrow-derived mesenchymal stromal cells.* Blood, 2011. **118**(2): p. 380-9.

122. Uy, G.L., et al., *Targeting bone marrow lymphoid niches in acute lymphoblastic leukemia.* Leuk Res, 2015. **39**(12): p. 1437-42.

123. Naderi, E.H., et al., *Bone marrow stroma-derived PGE2 protects BCP-ALL cells from DNA damage-induced p53 accumulation and cell death.* Mol Cancer, 2015. **14**: p. 14.

124. Veiga, J.P., et al., *Leukemia-stimulated bone marrow endothelium promotes leukemia cell survival.* Exp Hematol, 2006. **34**(5): p. 610-21.

125. Boyerinas, B., et al., *Adhesion to osteopontin in the bone marrow niche regulates lymphoblastic leukemia cell dormancy.* Blood, 2013. **121**(24): p. 4821-31.

126. Shiozawa, Y., E.A. Pedersen, and R.S. Taichman, *GAS6/Mer axis regulates the homing and survival of the E2A/PBX1-positive B-cell precursor acute lymphoblastic leukemia in the bone marrow niche.* Exp Hematol, 2010. **38**(2): p. 132-40.

127. Quagliano, A., A. Gopalakrishnapillai, and S.P. Barwe, *Epigenetic drug combination overcomes osteoblast-induced chemoprotection in pediatric acute lymphoid leukemia.* Leuk Res, 2017. **56**: p. 36-43.

128. Jacamo, R., et al., *Reciprocal leukemia-stroma VCAM-1/VLA-4-dependent activation of NF-kappaB mediates chemoresistance.* Blood, 2014. **123**(17): p. 2691-702.

129. Hsieh, Y.T., et al., *Integrin alpha4 blockade sensitizes drug resistant pre-B acute lymphoblastic leukemia to chemotherapy.* Blood, 2013. **121**(10): p. 1814-8.

130. Shalapour, S., et al., *High VLA-4 expression is associated with adverse outcome and distinct gene expression changes in childhood B-cell precursor acute lymphoblastic leukemia at first relapse.* Haematologica, 2011. **96**(11): p. 1627-35.

131. Bertrand, F.E., et al., *Inhibition of PI3K, mTOR and MEK signaling pathways promotes rapid apoptosis in B-lineage ALL in the presence of stromal cell support.* Leukemia, 2005. **19**(1): p. 98-102.

132. Bradstock, K.F., et al., *Effects of the chemokine stromal cell-derived factor-1 on the migration and localization of precursor-B acute lymphoblastic leukemia cells within bone marrow stromal layers.* Leukemia, 2000. **14**(5): p. 882-8.

133. Shen, W., et al., *The chemokine receptor CXCR4 enhances integrin-mediated in vitro adhesion and facilitates engraftment of leukemic precursor-B cells in the bone marrow.* Exp Hematol, 2001. **29**(12): p. 1439-47.

134. van den Berk, L.C., et al., *Disturbed CXCR4/CXCL12 axis in paediatric precursor B-cell acute lymphoblastic leukaemia.* Br J Haematol, 2014. **166**(2): p. 240-9.

135. Sison, E.A., et al., *Plerixafor as a chemosensitizing agent in pediatric acute lymphoblastic leukemia: efficacy and potential mechanisms of resistance to CXCR4 inhibition.* Oncotarget, 2014. **5**(19): p. 8947-58.

136. Juarez, J., et al., *Effects of inhibitors of the chemokine receptor CXCR4 on acute lymphoblastic leukemia cells in vitro.* Leukemia, 2003. **17**(7): p. 1294-300.

137. Cooper, T.M., et al., *A phase 1 study of the CXCR4 antagonist plerixafor in combination with high-dose cytarabine and etoposide in children with relapsed or refractory acute leukemias or myelodysplastic syndrome: A Pediatric Oncology Experimental Therapeutics Investigators' Consortium study (POE 10-03).* Pediatr Blood Cancer, 2017. **64**(8).

138. Yamamoto-Sugitani, M., et al., *Galectin-3 (Gal-3) induced by leukemia microenvironment promotes drug resistance and bone marrow lodgment in chronic myelogenous leukemia.* Proc Natl Acad Sci U S A, 2011. **108**(42): p. 17468-73.

139. Fei, F., et al., *B-cell precursor acute lymphoblastic leukemia and stromal cells communicate through Galectin-3.* Oncotarget, 2015. **6**(13): p. 11378-94.

140. Hu, K., et al., *Galectin-3 mediates bone marrow microenvironment-induced drug resistance in acute leukemia cells via Wnt/beta-catenin signaling pathway.* J Hematol Oncol, 2015. **8**: p. 1.

141. Yang, Y., et al., *Wnt pathway contributes to the protection by bone marrow stromal cells of acute lymphoblastic leukemia cells and is a potential therapeutic target.* Cancer Lett, 2013. **333**(1): p. 9-17.

142. Streetly, M.J., et al., *GCS-100, a novel galectin-3 antagonist, modulates MCL-1, NOXA, and cell cycle to induce myeloma cell death.* Blood, 2010. **115**(19): p. 3939-48.

143. Paz, H., et al., *Treatment of B-cell precursor acute lymphoblastic leukemia with the Galectin-1 inhibitor PTX008.* J Exp Clin Cancer Res, 2018. **37**(1): p. 67.

144. Iwamoto, S., et al., *Mesenchymal cells regulate the response of acute lymphoblastic leukemia cells to asparaginase.* J Clin Invest, 2007. **117**(4): p. 1049-57.

145. Ehsanipour, E.A., et al., *Adipocytes cause leukemia cell resistance to L-asparaginase via release of glutamine.* Cancer Res, 2013. **73**(10): p. 2998-3006.

146. Butturini, A.M., et al., *Obesity and outcome in pediatric acute lymphoblastic leukemia.* J Clin Oncol, 2007. **25**(15): p. 2063-9.

147. Laranjeira, A.B., et al., *IGFBP7 participates in the reciprocal interaction between acute lymphoblastic leukemia and BM stromal cells and in leukemia resistance to asparaginase.* Leukemia, 2012. **26**(5): p. 1001-11.

148. Pallasch, C.P., et al., *Sensitizing protective tumor microenvironments to antibody-mediated therapy.* Cell, 2014. **156**(3): p. 590-602.

149. Zeng, Z., et al., *High-throughput profiling of signaling networks identifies mechanism-based combination therapy to eliminate microenvironmental resistance in acute myeloid leukemia.* Haematologica, 2017. **102**(9): p. 1537-1548.

150. Conforti, A., et al., *Biological, functional and genetic characterization of bone marrow-derived mesenchymal stromal cells from pediatric patients affected by acute lymphoblastic leukemia.* PLoS One, 2013. **8**(11): p. e76989.

151. Poon, Z., et al., *Bone marrow MSCs in MDS: contribution towards dysfunctional hematopoiesis and potential targets for disease response to hypomethylating therapy.* Leukemia, 2019. **33**(6): p. 1487-1500.

152. Usmani, S., et al., *Support of acute lymphoblastic leukemia cells by nonmalignant bone marrow stromal cells.* Oncol Lett, 2019. **17**(6): p. 5039-5049.

153. Paggetti, J., et al., *Exosomes released by chronic lymphocytic leukemia cells induce the transition of stromal cells into cancer-associated fibroblasts.* Blood, 2015. **126**(9): p. 1106-17.

154. Kumar, B., et al., *Acute myeloid leukemia transforms the bone marrow niche into a leukemia-permissive microenvironment through exosome secretion.* Leukemia, 2018. **32**(3): p. 575-587.

155. Umezu, T., et al., *Leukemia cell to endothelial cell communication via exosomal miRNAs.* Oncogene, 2013. **32**(22): p. 2747-55.

156. Johnson, S.M., et al., *Metabolic reprogramming of bone marrow stromal cells by leukemic extracellular vesicles in acute lymphoblastic leukemia.* Blood, 2016. **128**(3): p. 453-6.

157. Liu, J., et al., *Stromal cell-mediated mitochondrial redox adaptation regulates drug resistance in childhood acute lymphoblastic leukemia.* Oncotarget, 2015. **6**(40): p. 43048-64.

158. Hulleman, E., et al., *Inhibition of glycolysis modulates prednisolone resistance in acute lymphoblastic leukemia cells.* Blood, 2009. **113**(9): p. 2014-21.

159. Xu, W., et al., *Characterization of prostate cancer cell progression in zebrafish xenograft model.* Int J Oncol, 2018. **52**(1): p. 252-260.

160. Huan, J., et al., *RNA trafficking by acute myelogenous leukemia exosomes.* Cancer Res, 2013. **73**(2): p. 918-29.

161. Thery, C., et al., *Isolation and characterization of exosomes from cell culture supernatants and biological fluids.* Curr Protoc Cell Biol, 2006. **Chapter 3**: p. Unit 3.22.

162. Mestdagh, P., et al., *A novel and universal method for microRNA RT-qPCR data normalization.* Genome Biol, 2009. **10**(6): p. R64.

163. Hemler, M.E., *Tetraspanin proteins mediate cellular penetration, invasion, and fusion events and define a novel type of membrane microdomain.* Annu Rev Cell Dev Biol, 2003. **19**: p. 397-422.

164. Peula, J.M., et al., *Covalent coupling of antibodies to aldehyde groups on polymer carriers.* Journal of Materials Science: Materials in Medicine, 1995. **6**(12): p. 779-785.

165. Chiba, M., M. Kimura, and S. Asari, *Exosomes secreted from human colorectal cancer cell lines contain mRNAs, microRNAs and natural antisense RNAs, that can transfer*

into the human hepatoma HepG2 and lung cancer A549 cell lines. Oncol Rep, 2012. **28**(5): p. 1551-8.

166. Ono, M., et al., *Exosomes from bone marrow mesenchymal stem cells contain a microRNA that promotes dormancy in metastatic breast cancer cells.* Sci Signal, 2014. **7**(332): p. ra63.

167. Dong, W., et al., *Diagnostic and predictive significance of serum microRNA-7 in esophageal squamous cell carcinoma.* Oncol Rep, 2016. **35**(3): p. 1449-56.

168. Hannafon, B.N., et al., *Plasma exosome microRNAs are indicative of breast cancer.* Breast Cancer Res, 2016. **18**(1): p. 90.

169. Zhuang, Z., C. Sun, and H. Gong, *High serum miR-484 expression is associated with the diagnosis and prognosis of patients with non-small cell lung cancer.* Exp Ther Med, 2019. **18**(5): p. 4095-4102.

170. Lu, X. and J. Lu, *The significance of detection of serum miR-423-5p and miR-484 for diagnosis of colorectal cancer.* Clin Lab, 2015. **61**(1-2): p. 187-90.

171. Li, A., et al., *MicroRNA array analysis finds elevated serum miR-1290 accurately distinguishes patients with low-stage pancreatic cancer from healthy and disease controls.* Clin Cancer Res, 2013. **19**(13): p. 3600-10.

172. Zearo, S., et al., *MicroRNA-484 is more highly expressed in serum of early breast cancer patients compared to healthy volunteers.* BMC Cancer, 2014. **14**: p. 200.

173. Kong, Q., et al., *Diagnostic Value of Serum hsa-mir-92a in Patients with Cervical Cancer.* Clin Lab, 2017. **63**(2): p. 335-340.

174. Liu, G.H., et al., *Serum miR-21 and miR-92a as biomarkers in the diagnosis and prognosis of colorectal cancer.* Tumour Biol, 2013. **34**(4): p. 2175-81.

175. Liu, H.N., et al., *Serum microRNA signatures and metabolomics have high diagnostic value in gastric cancer.* BMC Cancer, 2018. **18**(1): p. 415.

176. Shin, V.Y., et al., *Circulating cell-free miRNAs as biomarker for triple-negative breast cancer.* Br J Cancer, 2015. **112**(11): p. 1751-9.

177. Zou, X., et al., *Identification of a six-miRNA panel in serum benefiting pancreatic cancer diagnosis.* Cancer Med, 2019. **8**(6): p. 2810-2822.

178. Li, M., et al., *Circulating miR-25-3p and miR-451a May Be Potential Biomarkers for the Diagnosis of Papillary Thyroid Carcinoma.* PLoS One, 2015. **10**(7): p. e0132403.

179. Fujiwara, T., et al., *Clinical significance of circulating miR-25-3p as a novel diagnostic and prognostic biomarker in osteosarcoma.* Oncotarget, 2017. **8**(20): p. 33375-33392.

180. Yang, Y., et al., *Interferon-microRNA signalling drives liver precancerous lesion formation and hepatocarcinogenesis.* Gut, 2016. **65**(7): p. 1186-201.

181. Vasyutina, E., et al., *The regulatory interaction of EVI1 with the TCL1A oncogene impacts cell survival and clinical outcome in CLL.* Leukemia, 2015. **29**(10): p. 2003-14.

182. Cui, J., et al., *Leukemia cell-derived microvesicles induce T cell exhaustion via miRNA delivery.* Oncoimmunology, 2018. **7**(7): p. e1448330.

Danksagung

An dieser Stelle möchte ich bei jedem Einzelnen bedanken, der mich bei dieser Dissertationsarbeit unterstützt hat.

Insbesondere gilt mein Dank folgenden Personen:

Mein Dank gilt zunächst meiner Betreuerin Dr. Vera Binder, für das Überlassen des Themas und der Betreuung der Arbeit. Insbesondere möchte ich mich bedanken für die allwöchentlichen lab meetings bis spät in die Nacht und die individuelle Förderung, sei es für Kongressteilnahmen oder interne Vorträge. Danke auch für das Vermitteln von Wissenschaft und dem Engagement beim Ausarbeiten des Manuskriptes.

Genauso danke ich meiner Doktormutter Professor Dr. Irmela Jeremias für die Betreuung der Arbeit. Danke für die Aufnahme des kleinen Binder-labs in den großen Kreis der AHS. Besonders Danke für die kritischen Kommentare, die in internen Meetings oft zu kurz kommen und zur wichtigen Reflexion über Herangehensweisen und Interpretationen geführt haben. Danke für die detaillierte und engagierte Überarbeitung der Arbeit.

Ich bedanke mich bei meinem Labor-Mitglied Anja Arner, PhD, die mich in den ersten Monaten in das Projekt eingearbeitet hat, und auch nachher stets in den meetings in meinem Projekt mitgedacht hat.

Vielen Dank an alle Mitglieder der Arbeitsgruppe AHS, für produktiven Input beim Forschen und sehr gute Stimmung bei der Arbeit. Insbesondere gilt mein Dank den PhD-Kandidaten in meinem Büro für die universelle Hilfsbereitschaft, auch bei kleinen Anliegen. Danke auch den Postdocs für methodische Unterstützung und den technicians, insbesondere Annette Frank und Miriam Krekel, für das Vorbereiten der Maus-Seren.

Vielen Dank an alle Zuständigen bei FöFoLe für die strukturelle Organisation und die finanzielle Förderung des Projektes.

Selbstverständlich danke ich meiner Familie und meinen Freunden für das Leben außerhalb von Labor und Studium. Danke FöFoLe-Vorlesungs-Team, und danke Flo für die Kaffeepausen.

Natürlich möchte ich mich bei allen Patientinnen und Patienten sowie deren Eltern bedanken; durch Ihr Einverständnis wird die Forschung erst ermöglicht.

Affidavit

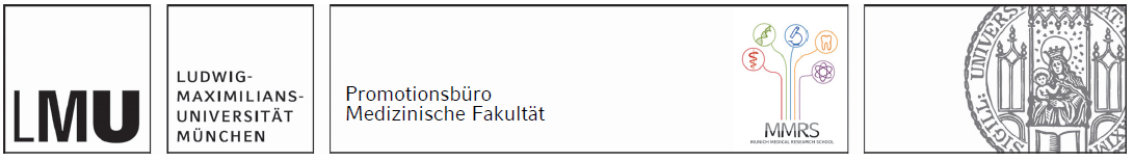

Eidesstattliche Versicherung

Bartholomé, Robert_____
Name, Vorname

Ich erkläre hiermit an Eides statt, dass ich die vorliegende Dissertation mit dem Titel:

Identification of circulation-derived exosomal microRNA candidates for liquid biopsy in pediatric acute lymphoblastic leukemia

selbständig verfasst, mich außer der angegebenen keiner weiteren Hilfsmittel bedient und alle Erkenntnisse, die aus dem Schrifttum ganz oder annähernd übernommen sind, als solche kenntlich gemacht und nach ihrer Herkunft unter Bezeichnung der Fundstelle einzeln nachgewiesen habe.

Ich erkläre des Weiteren, dass die hier vorgelegte Dissertation nicht in gleicher oder in ähnlicher Form bei einer anderen Stelle zur Erlangung eines akademischen Grades eingereicht wurde.

Solothurn, 02.12.2022_____
Ort, Datum

Robert Bartholomé_____
Unterschrift Doktorand